Sustainable urea production via CO_2 capture from cement plants

A techno-economic analysis with focus on process heat integration and electrification

Asgharian, Hossein; Duran, Albert Pujol; Yahyaee, Ali; Pignataro, Valeria; Nielsen, Mads Pagh; Iov, Florin; Liso, Vincenzo

DOI
10.1016/j.ijhydene.2025.150154

Publication date
2025

Document Version
Final published version

Published in
International Journal of Hydrogen Energy

International Journal of Hydrogen Energy 151 (2025) 150154

Contents lists available at ScienceDirect

International Journal of Hydrogen Energy

journal homepage: www.elsevier.com/locate/he

Sustainable urea production via CO_2 capture from cement plants: A techno-economic analysis with focus on process heat integration and electrification

Hossein Asgharian [a,*], Albert Pujol Duran [a], Ali Yahyaee [b], Valeria Pignataro [c], Mads Pagh Nielsen [a], Florin Iov [a], Vincenzo Liso [a]

[a] Department of AAU Energy, Aalborg University, Pontoppidanstræde 111, 9220 Aalborg, Denmark
[b] Process & Energy, Mechanical Engineering, Delft University of Technology, Leeghwaterstraat 39, 2628 CB Delft, the Netherlands
[c] University of Pisa, Department of Energy, Systems, Territory and Construction Engineering, Pisa, Italy

ARTICLE INFO

Keywords:
Sustainable urea production
CO_2 capture and utilization
Techno-economic analysis
Heat integration
System level modelling

ABSTRACT

Urea, a key derivative of ammonia, is widely used in agriculture and has a significant impact on food security. This study evaluates a sustainable urea production pathway that utilizes hydrogen generated from water electrolysis for green ammonia synthesis and CO_2 captured from a cement plant using an MEA-based process. This study employed Aspen Plus V12.1 and MATLAB to develop rigorous system-level models of all subsystems involved in the sustainable urea production process. These subsystems include a cryogenic air separation unit (CASU), a modular system of alkaline electrolysers (AEL), a green Haber-Bosch (HB) process, an MEA-based CO_2 capture system, and the Stamicarbon process. To enhance the energy efficiency and cost-effectiveness of urea production, waste heat generated during green ammonia synthesis in the HB process was integrated into the stripper column of the MEA-based CO_2 capture system for solvent regeneration. A detailed economic analysis was conducted to assess the impact of this heat integration (HI) on reducing the CO_2 capture costs and, consequently, the overall urea production costs. Additionally, several heat supply scenarios were evaluated to meet the heat demand of the CO_2 stripper column in the Stamicarbon process. These included natural gas combustion, a cascade heat pump (HP), and natural gas combustion integrated with a cryogenic CO_2 capture (CCC) system. The results indicated that HI significantly decreases both the energy penalty and costs of the MEA-based CO_2 capture process, reducing the CO_2 capture costs by 41.27 % in 2024 and lowering the energy penalty by 50.40 %. Among the scenarios investigated, the cascade HP with HI proved to be the most cost-effective option for urea production. Additionally, electricity costs for operating the modular alkaline electrolyzers (AEL) dominate the sustainable urea production expenses, with 88.07 %–91.26 % of electricity costs allocated to AEL, depending on the selected production scenario. The modular AEL also represents the largest share of initial investment costs, accounting for 90.62 % of total capital expenditures in the urea production process.

Nomenclature

a	Activity	CCC	Cryogenic CO_2 capture process
E	Activation energy (cal/mol)	HB	Haber-Bosch
F	Faraday constant (C/mol)	HI	Heat integration
i	Current density (A/m^2)	HP	Heat pump
I	Current (A)	HPC	High pressure column
k	Kinetic constant (kmol/m^3. s)	LPC	Low pressure column
k_0	Pre-exponential factor (kmol/m^3. s)	MEA	Monoethanolamine
k_r	Kinetic constant of the reverse reaction [−]	PEM	Proton exchange membrane
K_a	Equilibrium constant [−]	SMR	Steam methane reforming
k_1	Equilibrium constant [−]	SOEC	Solid oxide electrolysers
k_2	Equilibrium constant [−]		
s	Semi-empirical parameter [−]		
n	Number of cells [−]		
$\dot{n}$	Hydrogen production (kmol/hr)		
P	Pressure (bar)		

(continued on next column)

(continued)

(continued on next page)

* Corresponding author.
E-mail address: hoas@energy.aau.dk (H. Asgharian).

https://doi.org/10.1016/j.ijhydene.2025.150154
Received 13 May 2025; Received in revised form 23 June 2025; Accepted 23 June 2025
Available online 30 June 2025

(*continued*)

r	Reaction rate (kmol.m^{-3}.hr^{-1})
R	Gas constant (J/(mol.K))
T	Temperature (K)
U	Voltage/overvoltage (V)
x	Mole fraction [−]
z	Number of moles of transferred electrons [−]
Greek letters	
β_1	Semi-empirical parameter (cm^2. A^{-1})
β_2	Semi-empirical parameter (cm^2. °C. A^{-1})
β_3	Semi-empirical parameter (cm^2. °C^2. A^{-1})
α_1	Semi-empirical parameter (Ω. cm^2)
α_2	Semi-empirical parameter (Ω. cm^2. °C^{-1})
η	Faraday efficiency [−]
Subscripts	
Act	Activation
ohm	Ohmic
Rev	Reversible
CARB	Ammonium carbamate
Abbreviations	
AEL	Alkaline electrolyser
CASU	Cryogenic air separation unit

1. Introduction

Urea has a high nitrogen content and excellent solubility, making it widely used in agriculture as one of the most popular nitrogen-based fertilizers [1]. Its role as a nitrogen carrier fertilizer is crucial for enhancing crop yields, supporting agriculture, and contributing to food production. As a result, its production is expected to increase from 234.41 million metric tons in 2022 to 300 million metric tons by 2030 [2]. Currently, urea production heavily relies on fossil fuels and SMR for ammonia synthesis. This method not only exhausts the fossil fuel reserves but also generates significant CO_2 emissions. It has been shown that producing 1 kg of hydrogen via the SMR results in the emission of 8.9 kg of CO_2 [3]. Hence, urea production is currently responsible for approximately 1.2 % of global CO_2 emissions [4]. Given the growing demand for urea, its contribution to CO_2 emissions is expected to increase in the future. Therefore, it is crucial to replace the current fossil fuel-dependent urea production methods with green and sustainable alternatives to achieve the CO_2 neutrality target by 2050.

Ammonia and CO_2 serve as the required feedstocks for urea production. For green urea production, CO_2 captured either from point sources or directly from atmospheric air reacts with green ammonia. Although 96 % of the hydrogen used in ammonia production currently comes from fossil fuels through SMR [5], alternative green methods are available, including biomass-based hydrogen generation, microbial hydrogen production, water electrolysis, thermolysis, and thermochemical cycles. However, among these various sustainable methods, water electrolysis has gained significant popularity for large-scale green hydrogen production. Three primary methods for producing green hydrogen via water electrolysis include the use of alkaline electrolysers, proton exchange membrane (PEM) electrolysers, and solid oxide electrolysers (SOEC) [6]. Mazzeo et al. [7] examined the use of alkaline electrolyzers powered by wind and solar photovoltaics for large-scale green hydrogen production. This study compared the performance of different renewable energy systems, including wind turbines, PV, and hybrid PV-wind turbines. Each energy system was designed with a peak capacity of 100 MW to power alkaline electrolysers with a capacity of 24 MW. The performance of these systems was evaluated across 28 locations worldwide, covering diverse climate conditions. This research provides essential guidelines for selecting suitable locations for establishing renewable energy systems based on PV, wind turbines, or hybrid PV-wind turbines to enable efficient green hydrogen production via alkaline electrolysers. Ehler et al. [8] further investigated the large-scale green hydrogen production using AEL from an industrial perspective, aiming to make green hydrogen more affordable in the future. The study emphasized that while energy efficiency is a key factor, it is not the only barrier to reducing the cost of green hydrogen production with AEL. They suggested that increasing the operating temperature of AEL to 120 °C, along with improving the conductivity and stability of diaphragm separators, could significantly enhance performance and cost-effectiveness.

Direct air capture (DAC) technologies, primarily based on aqueous or solid sorbent processes, are designed to capture CO_2 directly from atmospheric air. These technologies are still in the early stages of development and are considered energy-intensive due to the challenge of capturing CO_2 from a highly diluted gas mixture. In addition to DAC technologies, other methods like pre-combustion, oxy-fuel combustion, and post-combustion CO_2 capture processes are employed to capture CO_2 with higher concentrations from point sources. Galusnyak et al. [9] assessed the technical and environmental implications of decarbonizing cement production using post-combustion CO_2 capture processes. Their study evaluated three post-combustion CO_2 capture technologies including chemical absorption using Methyl-Diethanolamine, solid adsorption via calcium looping, and membrane-based processes to capture 90 % of the CO_2 in flue gas emissions from a cement factory. The results indicated that integrating post-combustion CO_2 capture methods in cement production can reduce the global warming potential by 69.91 %–76.74 %, with the calcium looping process showing the highest efficiency.

Alfian et al. [10] also carried out a multi-objective optimization for the production of green urea to identify the most cost-effective strategy with the lowest environmental impacts for the period of 2020–2050, taking into account the projected prices for components and feedstocks required by each technology. The study's results indicated that replacing the conventional fossil fuel-based methods with green production methods can significantly reduce both CO_2 emissions and production costs. Additionally, the analysis showed that from 2020 to 2035, biomass gasification offers the lowest CO_2 emissions and operating costs for urea production. However, from 2040 to 2050, a combined process using biomass gasification and water electrolysis powered by PV is the optimal approach in terms of minimizing both operating costs and CO_2 emissions. Gyanwali et al. [11] presents a techno-economic analysis of green urea production in Nepal, using municipal solid waste and hydropower to produce sustainable urea. They modeled the process in Aspen Plus, designing a system that operates with 230 MW of power, 740 tons of organic waste per day, and 220 tons of combustible waste per day to produce 661 tons of urea daily. The analysis showed that the plant's total CO_2 emissions are limited to 32.74 kg per ton of urea produced, which is 29 times lower than emissions from conventional fossil fuel-based methods. Devkata et al. [4] conducted a techno-economic and environmental analysis of green urea production using Aspen Plus and MATLAB. In their study, green hydrogen was supplied via a water electrolysis process, CO_2 was captured from a cement plant, and hydropower provided the necessary energy for the production process. The analysis indicated that the producing urea at a capacity of 0.22 million tons per year requires 8.18×10^6 GJ energy annually. The study also found that the levelized cost of urea was 570.96 USD/ton, which is 62.2 % higher than that of conventional fossil fuel-based methods. Zhang et al. [12] further evaluated a green urea production process powered entirely by renewable energy sources. They introduced a novel method combining biomass and power-to-ammonia processes, capable of fully converting the CO_2 into urea. The study found that this proposed process achieves an energy efficiency of 53 %, significantly higher than the 39 % efficiency of the conventional biomass-to-urea process. However, the economic analysis revealed that the levelized costs of the proposed method are 58–87 % higher

compared to the biomass-to-urea process, primarily due to the elevated power consumption involved. Fernando et al. [13] evaluated the power-to-green urea concept for a plant with a capacity of 13,000 million tons per year. Their study found that the system's efficiency, powered by PV, was 7.9 %, with a specific energy consumption calculated at 109 GJ per million tons of green urea produced. Kashyap et al. [14] also assessed the techno-economic viability of CO_2 utilization for generation of green urea. Their study considered Monoethanolamine (MEA) scrubbing with a capacity of 0.5 million tons of CO_2 annually to capture CO_2 from 32 major cement plants in India, providing the necessary feedstock for green urea production. The results indicated that this CO_2 capture and utilization (CCUS) approach could potentially reduce CO_2 emissions from the Indian cement industry by 12.4 % if implemented across these 32 plants. Additionally, the study showed that this CCUS technology could offer a six-year payback period with a 16.7 % return on investment.

Although various aspects of urea production have been studied in the literature, to the best of our knowledge, the integration of waste heat from the ammonia synthesis reactor into the stripper column of the MEA-based CO_2 capture system, aimed at reducing the power consumption, lowering CO_2 capture and urea production costs, and improving the overall energy efficiency of the process, has not yet been investigated. Furthermore, the impact of different heat supply scenarios for the CO_2 stripper column has not been explored, particularly with respect to fuel costs and CO_2 emission costs (in the case of natural gas combustion), and electricity costs associated with the use of a cascade HP and the CCC process.

This study offers a thorough techno-economic analysis for production of sustainable urea using Aspen Plus V.12 and MATLAB. Green hydrogen is supplied from an AEL system, while CO_2 is captured from a cement factory in Denmark using an MEA-based CO_2 capture process. For the first time, this study evaluates an integrated energy conversion system that considers all sub-systems involved in the urea production process and integrates the heat from the ammonia production reactor in the Green HB process into the MEA-based CO_2 capture process. This integration provides the necessary heat duty for regeneration of the solvent in the stripper column, allowing for an assessment of its impact on the overall urea production process and its associated costs. Additionally, the study examines how this HI affects the energy penalty and costs of the MEA-based CO_2 capture process. To meet the heat demand of the Stamicarbon process, various scenarios were explored, including natural gas combustion, a cascade HP, and natural gas combustion integrated with a CCC process. The impact of these scenarios on CO_2 emissions, CO_2 emission costs, and urea production costs was also investigated.

2. Methodology

This section outlines the process flow diagram for urea production, incorporating nitrogen generated from a CASU, green hydrogen supplied by an AEL modular system, and ammonia produced via the green HB process. Additionally, the CO_2 captured from a cement factory in Denmark using MEA scrubbing is reacted with green ammonia to produce urea via the Stamicarbon process, where the heat required for the

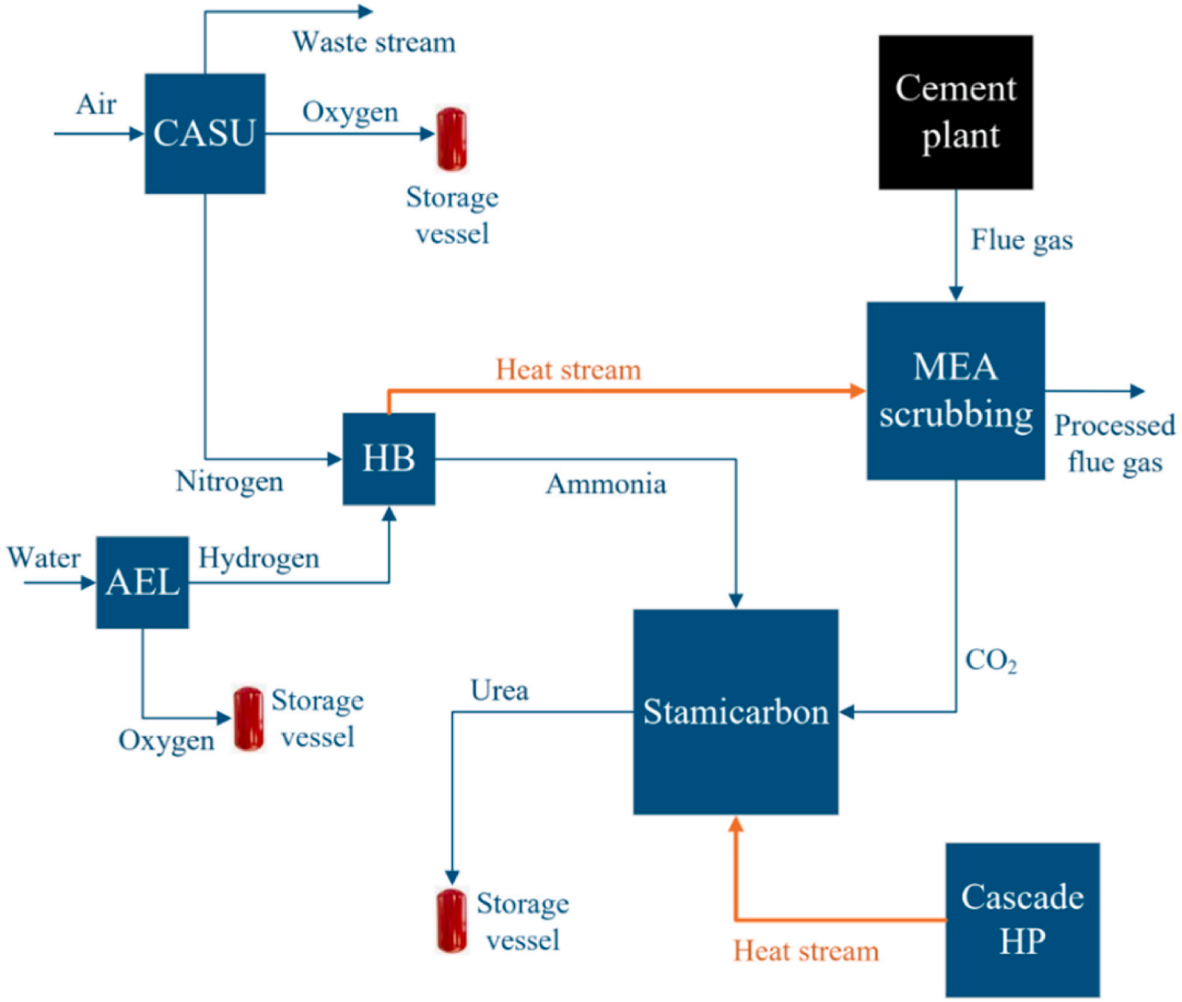

Fig. 1. Conceptual study diagram of the sustainable urea production process.

CO_2 stripper column is supplied by a cascade HP. This process flow incorporates an efficient HI from the ammonia production reactor to the CO_2 capture system in order to minimize the power demand of the MEA scrubbing process, which is known to be energy intensive. These six subsystems used in the sustainable urea production process along the main inputs and outputs of the subsystems along with the HI are shown in Fig. 1 which provides a conceptual study diagram of the green urea production process. Furthermore, this section elaborates on the models developed in MATLAB and Aspen Plus for the AEL modular systems, ammonia production, MEA scrubbing process, and Stamicarbon process for sustainable urea production process [15].

2.1. Process description

Fig. 2 presents the simplified process flow diagram, illustrating the six subsystems involved in sustainable urea production. As can be seen, the electrolyte, an aqueous solution containing 25 % by weight of potassium hydroxide (KOH), enters the AEL module (state 7), consisting of 180 stacks. As a result, the deionized water in the solution decomposes into oxygen (state 8) and hydrogen (state 18), with the temperature rising primarily due to irreversibilities, that occur when the cell voltage exceeds the thermoneutral voltage [16]. Consequently, a cooling system is required to maintain the electrolyte's operating temperature at 70 °C. The generated oxygen stream is sent to a flash tank to remove its electrolyte content (state 16), and a make-up deionized water stream (state 15) is mixed with the separated electrolyte leaving the flash tank from the bottom to compensate for the decomposed water in the modular electrolyzer system. The separated oxygen stream exiting the flash tank from the top (state 9) is water-cooled and flashed again to further purify it by separating its water content (state 13). The high-purity oxygen stream is then compressed and stored in a tank (state 12). Similarly, the hydrogen stream leaving the modular AEL is sent to a flash tank to remove its electrolyte content. The separated electrolyte (state 19) exits from the bottom and is subsequently via a pump (state 20) and mixed with the separated electrolyte from the oxygen stream (state 17). The resulting electrolyte stream is cooled and returned to the modular AEL system, while the hydrogen stream exiting the flash tank from the top (state 22) is also cooled (state 23), with its water content separated in a flash tank (state 24). The high-purity hydrogen stream (state 25) is compressed (state 26) and then mixed with the nitrogen stream supplied by the CASU.

Within the CASU, dried air (state 27), composed of 78.1 % nitrogen, 20.95 % oxygen, and 0.95 % argon, is compressed to 6 bars (state 28) and then water-cooled (state 29). The pressurized and cooled air stream is split into two streams: a minor stream that is further pressurized to higher pressures and a major stream. Both streams are then cooled to an extremely low temperature of −166 °C (states 34 and 36) using a multi-stream heat exchanger. As a result, the minor stream is liquefied, expanded to 1.35 bars (state 35), and then introduced into the low-pressure column (LPC). This expansion leads to a substantial decrease in the air stream temperature due to the Joule–Thomson effect, providing the necessary cooling and refrigeration to maintain cryogenic conditions in the LPC, which are essential for the condensation of oxygen and its separation from nitrogen [17]. The major stream is sent directly to the high-pressure column (HPC). A rich nitrogen stream exits the HPC from the top (state 37), and it is liquefied in a condenser (state 38), and partially recycled to the HPC (state 39), while the remainder is sent to the LPC after expansion to 1.35 bar (state 41). A rich nitrogen stream leaving the HPC bottom (state 42) is also expanded to 1.35 bar and directed to the LPC (state 43). Since oxygen has the highest boiling point among the components present in air [17], an oxygen-rich liquid stream exits the LPC from the bottom (state 46), is heated in the reboiler,

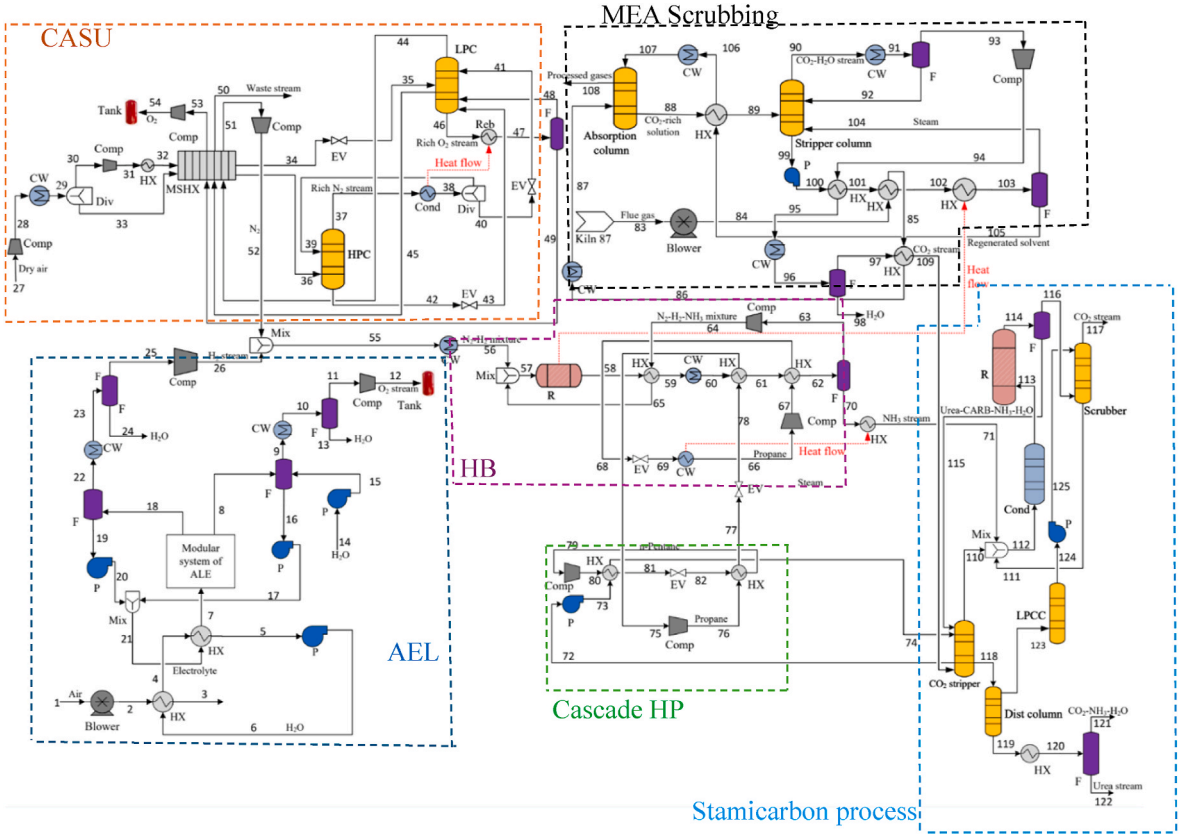

Fig. 2. Simplified process flow diagram of the urea production process (P: Pump, HX: Heat exchanger, F: Flash, R: Reactor, LPC: Low pressure column, HPC: High pressure column, CW: Cooling water, EV: Expansion valve, Div: Divider, Reb: Reboiler, Cond: Condenser, Comp: Compressor, Dist column: Distillation column, MSHX: Multi-stream heat exchanger, Mix: Mixer, LPCC: Low pressure carbamate condenser).

and then directed to a flash tank (state 47). The liquid oxygen stream leaves from the bottom (state 49) and is sent to the multi-stream heat exchanger, while the vapor stream (state 48) is recycled to the LPC. The nitrogen-rich vapor stream at extremely low temperatures exits the LPC from the top (state 44) and is routed to the multi-stream heat exchanger. A waste stream (state 45) also exits the LPC and is directed to the heat exchanger. The incoming air streams are cooled, raising the temperatures of the liquid oxygen stream, vapor nitrogen stream, and waste vapor stream to match the ambient temperature (states 32 and 33). The produced oxygen stream is compressed and stored in a tank (state 54), while the waste stream (state 50) is vented to the atmosphere, and the nitrogen stream is compressed (state 52), mixed with hydrogen (state 55), cooled to 450 °C (state 56), and directed to the green HB process for ammonia production.

An isothermal ammonia production reactor converts nitrogen and hydrogen into ammonia, utilizing the heat from the exothermic reaction to regenerate the solvent in the MEA scrubbing process. The mixed reactants with traces of water, oxygen, and argon enter the reactor after mixing with unreacted gases (state 57). The ammonia-rich product stream exits the reactor (state 58), heats the unreacted gas mixture (state 64), undergoes further cooling via water cooling (state 60), and is then cooled using the evaporator from the light hydrocarbon cycle of the cascade HP (state 61). The stream is cooled to −18 °C via a vapor compression refrigeration cycle to condense ammonia and then enters a flash tank (state 62) to separate the liquefied ammonia (state 70) from unreacted gases (state 63), which are pressurized (state 64) and recycled back to the reactor after gaining heat from the product stream (state 65). Although the ammonia stream entering the flash tank could be condensed at a higher temperature due to its elevated pressure (138.775 bar), which would reduce the chiller's power consumption, this study adopts a condensation temperature of −18 °C to maximize the purity of the produced ammonia and minimize the flow rate of the recycled stream by condensing more ammonia at lower temperatures. This approach not only reduces the power consumption of the compressor used to pressurize the recycled stream but also enhances the ammonia production in the reactor by lowering the gas hourly space velocity followed by increasing the residence time and reducing the ammonia concentration in the reactor's inlet stream.

In the urea production process, an MEA scrubbing system is employed to capture CO_2 from a cement factory in Denmark, providing a sustainable source of CO_2 as a reactant for the urea production plant. As shown in the figure, the flue gas is pressurized by a blower to 1.2832 bar (state 84) to compensate for the pressure drops in the CO_2 capture process. The flue gas thermal energy is then utilized to partially regenerate the solvent by increasing its temperature (state 85), after which the flue gas is further cooled (state 86) by heating the CO_2 stream to 100 °C which is the required temperature for the Stamicarbon process. It is then water-cooled and directed to the bottom of the absorption column (state 87). Inside the absorption column, the aqueous solvent (state 107) enters from the top and flows downward. Through liquid-gas contact, CO_2 is chemically absorbed and removed from the flue gas. As a result, the CO_2-depleted gas mixture exits from the top (state 108), while the CO_2-rich solution exits from the bottom (state 88) at a slightly higher temperature due to the exothermic absorption reaction. Before being fed into the stripper column, the CO_2-rich solution is preheated (state 89) by cooling the hot lean solvent (state 106). In the stripper column, the solution is heated to release the absorbed CO_2 and regenerate the solvent. Similar to Ref. [18], this study heats the CO_2-rich solution to 103.6 °C (state 103) for solvent regeneration. The main reason for selecting a comparatively low desorption temperature is to reduce the risk of thermal degradation of the solvent and extend its operational lifetime [19]. However, as seen in Fig. 2, the solvent temperature is gradually increased in several steps using the heat from the flue gas, compressed CO_2 stream, and the exothermic ammonia production reactor. The CO_2 stream leaving the stripper column (state 90) is water-cooled (state 91) and then compressed to 139.15 bar (state 94) to meet the pressure requirements for the Stamicarbon, raising its temperature to 544 °C. This high-temperature CO_2 is then used to heat the CO_2-rich solution before being water-cooled (state 96) and separated from its water content (state 98) in a flash tank. Finally, the CO_2 stream is reheated using the heat of flue gas and directed to the Stamicarbon process for the urea production (state 109). It is worth noting that the MEA scrubbing process results in water and MEA losses via streams 108 and 94. Therefore, a make-up stream of water and MEA is required prior to being introduced into the absorption column. However, this stream is not shown in Fig. 2 to avoid complexity.

The urea manufacturing process starts with liquified ammonia (state70) being pressurized to 137 bars before entering the high-pressure carbamate condenser (state 71). Simultaneously, CO_2 coming from the MEA scrubbing section (state 109) is fed to the CO_2 stripper at 100 °C. Within the stripper, the rising CO_2 gas counter currently strips the urea solution falling through the tubes, decomposing unreacted ammonium carbamate into NH_3 and CO_2. This vapor stream, along with the liquid ammonia enters the carbamate condenser. There, some NH_3 and CO_2 react exothermically (141.50 °C and 137 bars) to form ammonium carbamate following reaction given by Equation (12). The resulting solution (state 113) then flows into an adiabatic reactor at a temperature of 183 °C, where further urea and water are produced (as shown by Equation (13)). Here, the residual NH_3 and CO_2 react to form ammonium carbamate, providing heat for the slightly endothermic urea formation reaction. The unreacted gases (state 113) exit the reactor top to the high-pressure scrubber. In the scrubber, NH_3 and CO_2 form ammonium carbamate (state 111), which is mixed with liquid ammonia and recycled to the urea reactor via the high-pressure carbamate condenser [20]. Inert gases (state 117) escape the system.

The stripper's bottom stream containing the urea solution (state 118) is depressurized to 4.5 bar and enters a low-pressure distillation column at a temperature of 135 °C, where ammonium carbamate decomposes into NH_3 and CO_2. This mixture (state 123) is sent to a low-pressure carbamate condenser to form ammonium carbamate (state 125). This stream is subsequently cooled, pumped to the high-pressure scrubber, and finally returned to the urea reactor. Finally, the urea-rich liquid (state 119) from the distillation column is further processed in a flash drum [21]. The resulting solution is sent to the drying and granulation plant, with energy requirements ranging from 0.15 to 0.46 $MWhr/ton_{urea}$ [22,23]. Nevertheless, this stage is not covered in this work. To achieve a reasonable reaction rate and maintain the liquid phase, elevated temperatures are necessary, particularly because pure ammonium carbamate melts at 153 °C. In addition, overall reaction from ammonia and carbon dioxide to urea is exothermic due to the large energy release in the first step. High pressures are also required to condense the gaseous reactants (NH_3 and CO_2) into the liquid phase at these temperatures. As a result, commercial urea synthesis plants typically operate at temperatures between 170 and 220 °C and pressures between 125 and 250 bar [24].

Table 1 summarizes the main process streams depicted in Fig. 2 and presents the mass and energy balances for the sustainable urea production process under study.

2.2. Model description

This section describes the models developed in Aspen Plus V12.1 and MATLAB to model the urea production process and conduct a thorough techno-economic analysis of the process. Hence, this section describes the models developed for AEL, green HB process, MEA scrubbing process, and the urea production process. The key assumptions used to develop the model in this study are listed in Table 2.

2.2.1. Modelling the AEL

Given that this study is concentrated on the techno-economic analysis of a sustainable urea production process, a simplified model for the AEL was utilized. Specifically, the stack of an alkaline electrolyzer was

Table 1
Material and energy balance summary of the urea production process shown in Fig. 2.

Stream number in Fig. 2	Temperature (°C)	Pressure (atm)	Mass flow (kg/hr)	Composition (mass fraction)										
				N_2	O_2	CO_2	H_2O	Argon	Ammonium carbamate	Urea	MEA	Tetrafluoropropane	NH_3	H_2
12 (O_2 stream)	81.13	29.6077	68884.46	0	0.9992	0	0.000786	0	0	0	0	0	0	0
26 (H_2 stream)	303.316	137.72514	8767.47	0	0	0	0.011	0	0	0	0	0	0	0.9887
27 (Dry air)	15	1	77539.95	0.7554	0.2315	0	0	0.0131	0	0	0	0	0	0
52 (N_2 stream)	974.674825	137.72514	40155.8	0.99985	6.195 × 1e-6	0	0	0.00014	0	0	0	0	0	0
54 (O_2 stream)	519.1392	29.6077	12429.21	1.29592 × 1e-6	0.993676	0	0	0.0063	0	0	0	0	0	0
56 (H_2–N_2 mixture)	450	137.67579	48972.33	0.8207366	5.0855 × 1e-6	0	0.002023126	0.00011767	0	0	0	0	0	0.17711745
58 (H_2–N_2–NH_3 mixture)	450	137.059	184774.3	0.5797324	9.574 × 1e-5	0	0.000536133	0.00089694	0	0	0	0	0.29828	0.120449376
64 (H_2–N_2–NH_3 mixture)	−17.5575	137.72514	135802	0.78798	0.00012838	0	9.192 × 1e-9	0.00117796	0	0	0	0	0.04697	0.163734246
71 (NH_3 stream)	35	136.91	48965	0.0022452	5.0846733 × 1e-6	0	0.002022823	0.00011765	0	0	0	0	0.99519	0.000418910
76 (Propane)	204.52875	26.646928	13708.55	0	0	0	0	0	0	0	0	1	0	0
79 (n-pentane)	95.2944	14.803849	11024.13	0	0	0	0	0	0	1	0	0	0	0
83 (flue gas)	131.68	1	330700	0.4777517	0.08304416	0.212114	0.227089653	0	0	0	0	0	0	0
90 (CO_2–H_2O)	90.508166865243	1.0856	111764.88508578	0.0003942	0.00012873	0.566175	0.432343193	0	0	0	0.00095832	0	0	0
104 (steam)	103.59792145	1.05626943005181	116213.49268	0	0	0.06703	0.922470729	0	0	0	0.01049856	0	0	0
108 (processed gases)	70.26745488	1	247872.4331	0.6372132	0.11073452	0.028289	0.223751280	0	0	0	1.18494 × 1e−05	0	0	0
109 (CO_2 stream)	100	137.28102	63641.06	0.0006944	0.00022713	0.990273	0.008805285	0	0	0	0	0	0	0
114 (urea-CARB–NH_3–H_2O)	183	136.465	266308.1	0.0005978	0.00010473	0.057612	0.159407895	2.675512 × 1e-5	0.2298844486	0.3148137477	0	0	0.237464275	8.75812613 × 1e-5
121 (CO_2–NH_3–H_2O)	85	1	67485.12	2.25304 × 1e-6	3.262043 × 1e-6	0.459886	0.194660889	0	0	0.0003420986	0	0	0.34510	0
122 (urea stream)	85	1	110662.4	3.12154 × 1e-12	3.843379 × 1e-11	0.000106	0.232584702	0	0	00.7555515968	0	0	0.01175	0

Table 2
Key assumptions and dimensions used in developing the models for sustainable urea production process

Parameter		Value
Pressure drops in heat exchangers		0.05 bar [25]
Compressors efficiency		90 % (polytropic using ASME method) [25]
Pressure drops in towers		0.0037 bar per stage [25]
Pumps efficiency		0.75 [26]
Minimum temperature approach in the heat exchanger		2 °C [25,27]
Modular AEL system	Number of cells in each AEL stacks	326 [28]
	Number of stacks in the AEL modular systems	180
	Cell area	2.66 m^2 [28]
Green HB process	Reactor size	Length: 7 m Diameter: 2.7 m
	Particle size for iron-based catalyst	3 mm
	Operating mode for the reactor	Isothermal operating condition at 450 °C with 139.5 bar inlet pressure
CASU	Number of stages for HPC	20
	Diameter of HPC	1.524 m
	HPC operating pressure	4.5 bar
	Number of stages for LPC	45
	Diameter of LPC	1.85 m
	LPC operating pressure	1.3 bar [29]
MEA-scrubbing process	Operating pressure of absorber column	Atmospheric pressure
	Number of stages for absorption column	36
	Diameter of absorption column	4.5–8 m
	Calculation type of absorber	Rate-based
	Number of stages for stripper column	23
	Diameter of stripper column	6.5 m
	Operating pressure of stripper column	Atmospheric pressure
	Calculation type of stripper column	Rate-based
Stamicarbon process	Operating mode for the reactor	Reactor with specified temperature profile with 138.274 bar inlet pressure
	Number of stages for scrubber	5
	Size of the reactor	Length: 28.956 m Diameter: 2.292 m
	Diameter of scrubber	4.9 m
	Calculation type of scrubber	Equilibrium

modeled from an electrochemical point of view in order to estimate the hydrogen production under constant and nominal operating conditions. The performance of an AEL can be effectively represented by its polarization curve, which provides the cell voltage value as described in Equation (1):

$$U_{cell}(T,p,i_{cell}) = U_{rev}(T,p) + U_{act}(T,i_{cell},\alpha_1,\alpha_2) + U_{ohm}(T,i_{cell},s,\beta_1,\beta_2,\beta_3) \quad (1)$$

The reversible voltage corresponds to the minimum voltage needed to trigger an electrochemical reaction under ideal conditions and can be obtained from the Nernst Equation. The other two terms in Equation (1) represent energy losses, and they are referred to as "overvoltages". In particular, the term U_{act} corresponds to activation overvoltage, which represents the energy losses resulting from surpassing the activation energy needed to initiate the electrochemical reactions. The Ohmic overvoltages, U_{ohm}, represents the voltage losses occurring within an electrochemical cell due to the electrical resistance of its components (membrane and electrolyte) [16]. Overvoltages can be expressed as a function of the stack operating temperature, the current density flowing through the cells, and several semi-empirical parameters ($\alpha_1,\alpha_2,s,\beta_1,\beta_2,\beta_3$) which are specific to the stack and are adjusted accordingly. In this study, the parameters provided by Sakas et al. [28]. In this case, the hydrogen production can be estimated as a function of the stack current as follows:

$$\dot{n}_{H_2} = \eta_F\left(I_{cell}/(zF)\right)n_c \quad (2)$$

Here, z denotes the number of moles of electrons exchanged in the reaction, while F is the Faraday constant, n_c is the number of cells within each stack, and η_F is the faradaic efficiency, which was considered constant and equal to 0.86 [28]. The operating pressure of the stack has been set at 16 bar, while the operating temperature is kept constant through a cooling system. It is important to note that the model developed in Aspen Plus V12.1 for the AEL system is based on an RStoic reactor, which uses the output from a mathematical model developed in MATLAB. The fractional conversion was calculated based on the hydrogen production rate from Equation (2) and the water flow rate in the electrolyte solution, which constitutes 75 wt% of the electrolyte stream. A system of 180 stacks, as evaluated in Ref. [28], was considered, using the same electrolyte composition and flow rate per stack. The hydrogen production rate and outlet electrolyte temperature obtained from the Aspen Plus model were found to be in exact agreement with the values reported in Ref. [28].

2.2.2. MEA scrubbing process

The MEA-based CO_2 capture process depicted in the process flow diagram (Fig. 2) consists of an absorber and stripper system designed to remove CO_2 from flue gas using aqueous MEA. Flue gas enters the absorber, where it contacts the MEA solution, leading to CO_2 absorption and the formation of rich amine. The cleaned flue gas exits the top, while the CO_2-laden MEA is pumped to the stripper after preheating via heat exchangers. In the stripper, heat is supplied, releasing CO_2 from the rich amine, regenerating lean MEA for recirculation to the absorber. The desorbed CO_2 exits the top of the stripper and undergoes cooling and compression before final delivery. Heat integration is optimized through multiple heat exchangers to improve energy efficiency. The modeling framework of the MEA-based CO_2 capture system integrates both equilibrium and kinetic mechanisms to accurately represent the absorption and desorption processes. The reaction models provide a robust basis for optimizing CO_2 removal efficiency and enhancing solvent recovery while ensuring a high level of process sustainability. Additionally, detailed column specifications and structured packing enhance the accuracy of the mass transfer predictions, contributing to improved process performance. The overall system ensures efficient CO_2 capture while maintaining solvent recovery and process sustainability.

2.2.2.1. Modeling of the absorber and stripper. The chemical processes occurring in the absorber and stripper are modeled using equilibrium and kinetic reactions to describe the CO_2 capture and release mechanisms. These reactions include acid-base equilibria, amine protonation, and the reversible formation and breakdown of carbamate and bicarbonate species.

2.2.2.1.1. Equilibrium reactions. The equilibrium reactions, which maintain the ionic balance in the aqueous phase, are modeled based on Gibbs free energy calculations. The primary equilibria reactions are given by Equations (3)–(5) as follows:

$$2H_2O \rightleftharpoons H_3O^+ + OH^- \text{ (Water autoionization)} \quad (3)$$

$$HCO_3^- + H_2O \rightleftharpoons CO_3^{2-} + H_3O^+ \text{ (Bicarbonate deprotonation)} \quad (4)$$

$MEA^+ + H_2O \rightleftharpoons MEA + H_3O^+$ (MEA^+ deprotonation) (5)

2.2.2.1.2. Kinetic reactions. The rate-based model considers the time-dependent absorption and desorption of CO_2 in the MEA solution. The key kinetic reactions include:

$CO_2 + OH^- \rightarrow HCO_3^-$ (Bicarbonate formation) (6)

$HCO_3^- \rightarrow CO_2 + OH^-$ (Bicarbonate decomposition) (7)

$MEA + CO_2 + H_2O \rightarrow MEACOO^- + H_3O^+$ (Carbamate formation) (8)

$MEACOO^- + H_3O^+ \rightarrow MEA + CO_2 + H_2O$ (Carbamate breakdown) (9)

The kinetic constants for reactions 6–9 are calculated using the Arrhenius equation as follows:

$$k(T) = k_o e^{-E/RT} \quad (10)$$

where k_o, E and R denote pre-exponential factor, activation energy in cal/mol, and the universal gas constant, respectively. Table 3 provides the kinetic parameters used for simulating reactions 4–7 in both the absorber and stripper columns.

The bicarbonate formation and decomposition reactions have identical kinetic parameters in both the absorber and stripper. Similarly, the carbamate formation reaction exhibits the same parameters in both units. However, the carbamate breakdown reaction differs significantly between the absorber and stripper due to the thermal conditions in the stripper. This difference accounts for the enhanced CO_2 desorption rate in the stripper, where heat energy facilitates the release of CO_2 from the rich amine solution.

2.2.2.2. Absorber and stripper column Configuration. The absorber and stripper columns are modeled using a rate-based approach to account for mass transfer limitations and reaction kinetics. The absorber consists of 36 stages and operates under vapor-liquid equilibrium conditions. Feed streams enter at different locations: flue gas at stage 6, lean amine at stage 36, and a water wash at stage 1. The absorber employs Mellapak structured packing (250Y).

The stripper is modeled using an equilibrium-based approach with 23 stages. Rich amine enters at stage 23, while the regenerated lean amine exits at the bottom, and desorbed CO_2 exits from the top. The column is also packed with Mellapak 250Y.

The absorber and stripper columns use structured packing to enhance mass transfer and minimize pressure drop. The absorber is divided into two sections, with a packing height of 5 m in the first section and 25 m in the second section, leading to an overall column diameter of 8 m at the bottom. The stripper consists of a single packed section spanning 19 m, with a column diameter of 6.5 m.

2.2.3. Kinetic model green HB process

This study examines ammonia synthesis over the Haldor Topsøe iron-based KM1 catalyst, utilizing the reaction rate from Equation (11) to model the exothermic ammonia production in the green Haber-Bosch process [3].

Table 3
The kinetic parameters for reactions occurring the absorber and stripper columns [30–32].

Reaction	k_o	E	Unit operation
4	1.33×10^{17}	13249 cal/mol	Absorber and stripper
5	6.63×10^{16}	25656.1 cal/mol	Absorber and stripper
6	3.02×10^{14}	9855.81 cal/mol	Absorber and stripper
7	5.52×10^{23}	16518 cal/mol	Absorber
7	6.499×10^{27}	22782.1 cal/mol	Stripper

$$r_{NH_3} = k_r \left(K_a{}^2 a_{N_2} \left(\frac{(a_{H_2})^3}{(a_{NH_3})^2} \right)^{0.5} - \left(\frac{(a_{NH_3})^2}{(a_{H_2})^3} \right)^{0.5} \right) \quad (11)$$

where r_{NH_3} is the rate of ammonia production in $kmol_{NH_3} m^{-3} hr^{-1}$, while k_r and K_a denote the kinetic constant associated with reverse reaction and the equilibrium constant, respectively. Additionally, a_i (i = H_2, N_2, and NH_3) represents the activity of the substances participating in the ammonia production reaction. These parameters are discussed in detail in referenced [33]. This study models the ammonia production reaction using a plug flow reactor based on the LHHW kinetic model. The calculation of kinetic parameters for modeling the ammonia production reactor is comprehensively discussed in the supplementary materials. The coefficients for the driving force constants are provided in Table S1, and the validation of the developed model is shown in Fig. S6.

2.2.4. Stamicarbon process for urea production

In the Stamicarbon process, CO_2 and NH_3 react at high temperatures and pressures to form ammonium carbamate, which is then dehydrated to produce urea. In this process, all ammonia exiting the synthesis section is redirected back to the reactor, ensuring nearly complete conversion of ammonia into urea [34]. The first reaction given by Equation (12) is highly exothermic and rapid, requiring immediate heat dissipation under sufficient pressure to condense the ammonia and carbon dioxide [21]. Inside the adiabatic urea generation reactor, the second endothermic reaction shown by Equation (13) occurs in the liquid phase, dehydrating the ammonium carbamate produced in the first reaction into urea. The significant exothermicity of the overall process presents opportunities for heat integration applications [20].

$$2NH_3 + CO_2 \leftrightarrow NH_2COONH_4 \Delta H = -100\ kJ/mol \quad (12)$$

$$NH_2COONH_4 \leftrightarrow UREA + H_2O \Delta H = 27.6\ kJ/mol \quad (13)$$

The modelling of the urea process is based on the works detailed in Refs. [20,21]. The model uses an RSTOIC block in Aspen Plus software to simulate the carbamate condenser, employing a power-law model to describe the reaction of CO_2 and NH_3 to form ammonium carbamate as given by Equation (12). The urea reactor itself is modeled using an RPLUG unit block operating at 138 bar and 167 °C, where both reactions 12 and 13 occur. The RSTOIC block has a reaction conversion of 38 % to represent typical process conditions where CO_2 reacts with NH_3 to produce ammonium carbamate [20]. The kinetic models for the reactions involved in the urea production process shown by Equations (12) and (13) are given as follows:

$$r_{CARB} = k_1 \left(x_{NH_3}^2 x_{CO_2} - \frac{x_{CARB}}{K_1} \right) \quad (14)$$

$$r_{UREA} = k_2 \left(x_{CARB} - \frac{x_{UREA} x_{H_2O}}{K_2} \right) \quad (15)$$

The reaction rate equations for urea formation are expressed in terms of mole fractions (x_i), with units of $kmol/s/m^3$. Kinetic factors k_1 and k_2, and equilibrium constants are derived from Refs. [15,35]. The kinetic parameters for modeling the urea production reactor are provided in Table S2 of the supplementary materials, and the validation of the developed model is presented in Fig. S7.

The flowsheets developed in Aspen Plus V12.1 to model the subsystems described above are presented in Fig. S1–S5 in the supplementary materials.

3. Results and discussion

This section outlines the findings from the techno-economic analysis of the urea production process. First, the results from modeling the subsystems of the urea production process are discussed, followed by the economic analysis results for the six scenarios. The six scenarios are

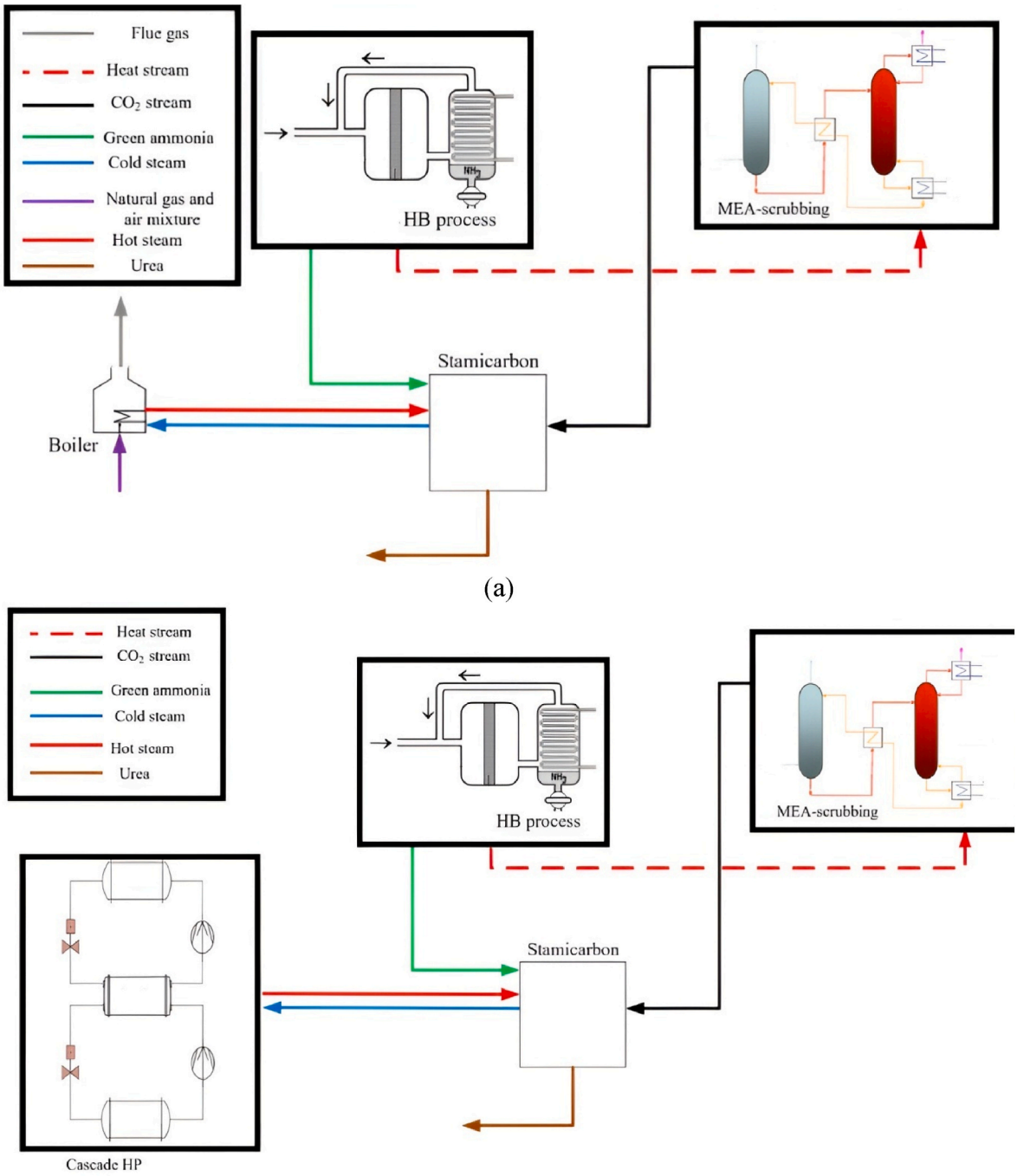

Fig. 3. Graphical diagram for six scenarios considered to calculate the urea production costs.

outlined below and illustrated in Fig. 3.

- With HI between the ammonia production reactor and the MEA scrubbing process, utilizing natural gas combustion to supply the required steam for the CO_2 stripper.
- With HI and the use of a cascade HP to supply the required steam for the CO_2 stripper.
- With HI and natural gas combustion supplying the required steam for the CO_2 stripper, integrated with a cryogenic CO_2 capture (CCC) process for CO_2 capture from natural gas combustion
- Without HI, using natural gas combustion to supply the required steam for the CO_2 stripper.
- Without HI, using a cascade HP to supply the required steam for the CO_2 stripper column in the Stamicarbon process.
- Without HI, using natural gas combustion to supply the required steam for the CO_2 stripper, integrated with the CCC process for CO_2 capture from natural gas combustion.

As mentioned in these scenarios, when using natural gas combustion to supply the required steam for the CO_2 stripper column within the

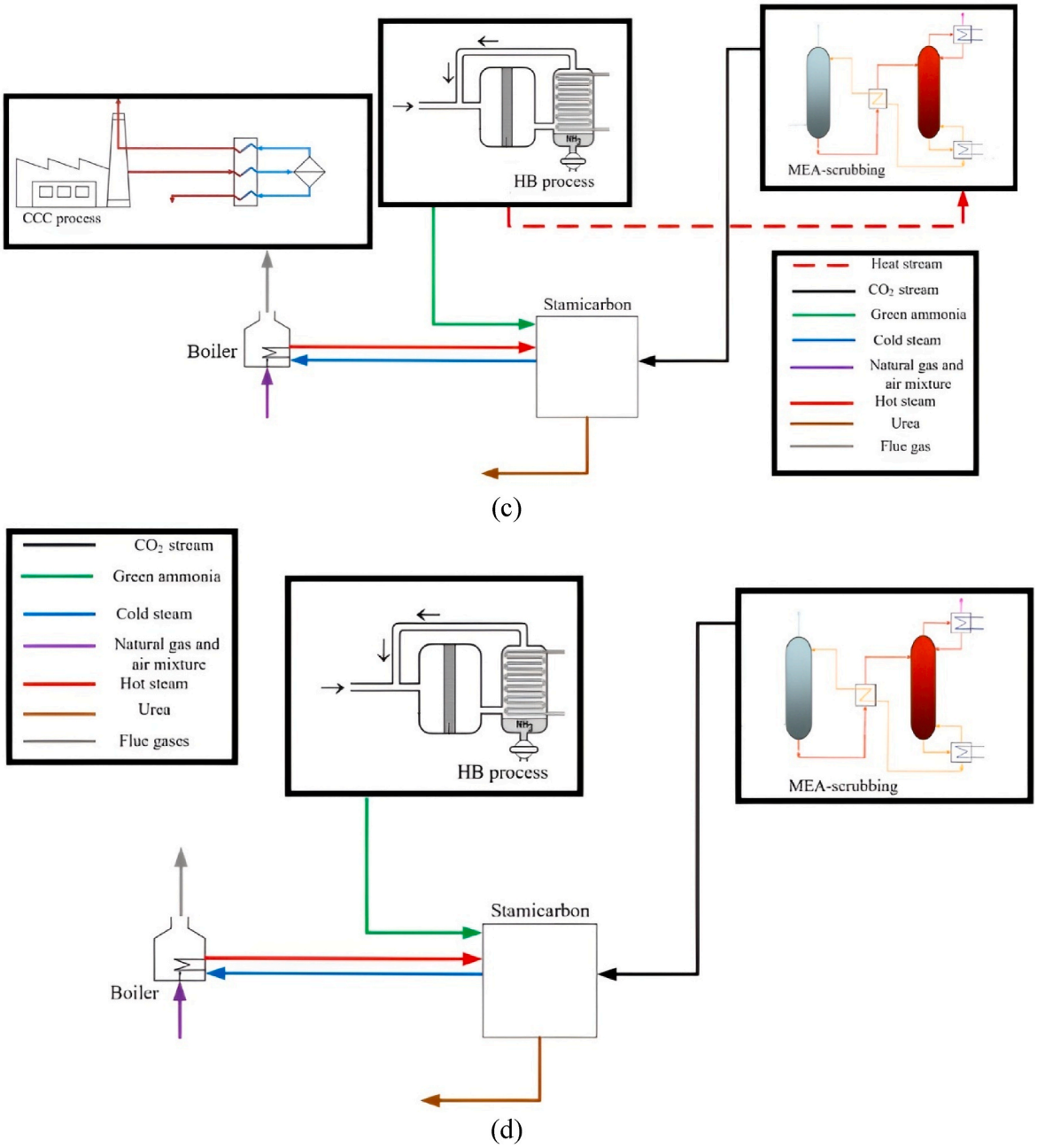

Fig. 3. (*continued*).

Stamicarbon process, this study will employ the CCC process to capture CO_2 from the flue gases generated during the combustion of natural gas, as this process has been proven to be highly energy-efficient and cost-effective. In this scenario, methane was assumed as the natural gas fuel. To supply the required heat for steam generation, a flow rate of 90.4 kmol/h of natural gas was combusted with 863 kmol/h of air, assuming 100 % combustion without the addition of excess air. The composition of the flue gas resulting from natural gas combustion is provided in Table S3 of the supplementary materials. The performance and operational characteristics of the CCC process are detailed in our previous study [27]. The CCC process modeled in this study operates with an energy penalty of 0.825 $\frac{MJ_e}{kg_{CO_2}}$ for capturing 90 % of the CO_2 from the flue gas emitted by natural gas combustion, which contains 9.47 % CO_2 on a wet basis. The distribution of power consumption across the components of the CCC process is presented in Fig. S9 of the supplementary materials. The primary focus of this study is to evaluate the six aforementioned scenarios to identify the most energy-efficient and cost-effective option for sustainable urea production.

3.1. Urea production process

Fig. 4 shows the variation of cell voltage versus current density for the utilized AEL at three temperatures: 50 °C, 70 °C, and 95 °C. As previously mentioned, a study by Sakas et al. [28] served as a reference for modeling the AEL, providing the operating parameters for a 3 MW AEL. A nominal current of 4569.88 A is supplied to each stack, resulting in a corresponding current density of 1718 A/m^2. As observed, operating the AEL modular system at higher temperatures not only enhances the electrode kinetics [36], but also reduces both the reversible potential and the Ohmic overvoltage [16]. This results in a decrease in the cell voltage, which subsequently leads to reduced power consumption.

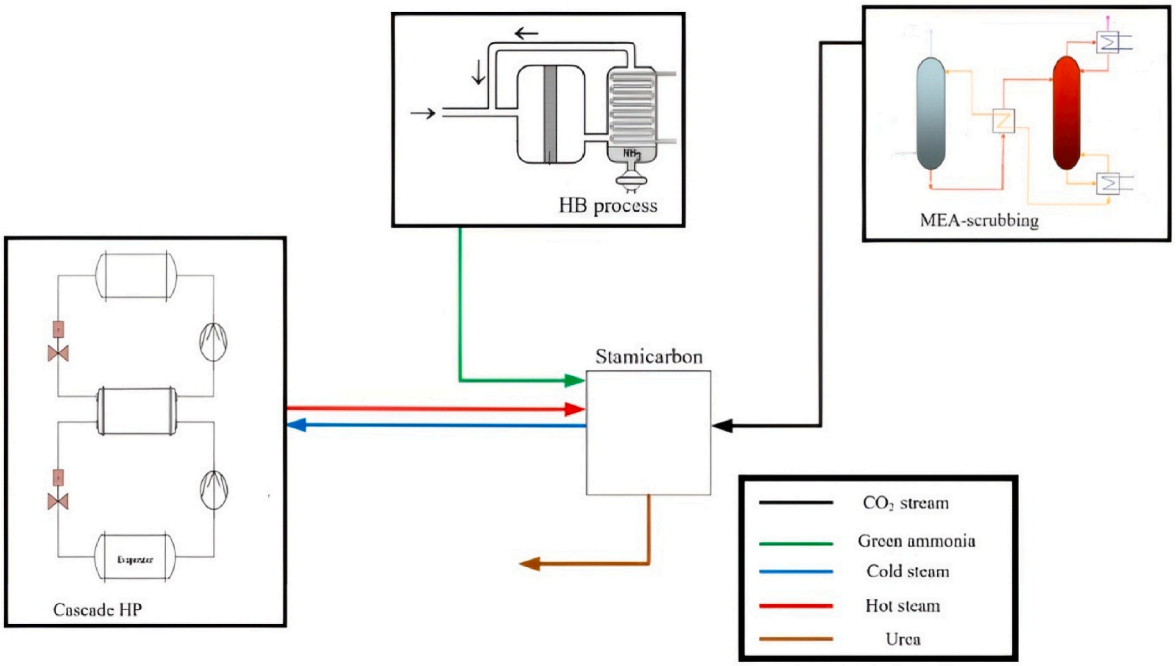

(e)

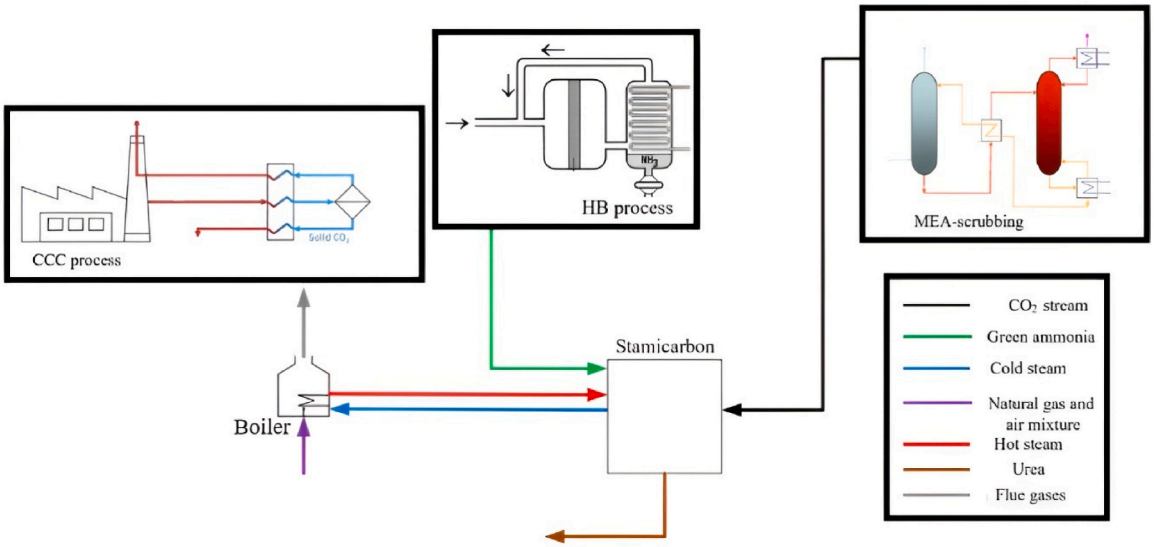

(f)

Fig. 3. (*continued*).

Specifically, increasing the temperature from 50 °C to 95 °C decreases power consumption by 2.45 %. However, operating at an excessively high temperature of 95 °C causes degradation of the catalyst material in the AEL modular system [37]. Therefore, in this study, an operating temperature of 70 °C was selected.

As shown in Fig. 5, the left axis indicates the reaction rate along the length of the reactor. At the reactor inlet, the ammonia generation rate is high due to the very low concentration of ammonia in the gas mixture, since only a trace amount is present from the recycled stream. However, as the gas mixture progresses through the reactor, the rate of ammonia production decreases. This decline is due to increasing the concentration of ammonia, which promotes the reverse reaction and suppresses the forward reaction for ammonia synthesis. As a result, near the reactor outlet, the reaction rate approaches to near zero values as chemical equilibrium is reached. The right axis of the plot shows the generation rate per unit length for ammonia, hydrogen, and nitrogen along the reactor. Since ammonia is produced in the reaction, it exhibits a positive generation rate, while hydrogen and nitrogen, being reactants, show negative generation rates since they are consumed. At the reactor inlet, where ammonia concentration is minimal, the forward reaction is highly favored, leading to a high rate of ammonia production and, consequently, high consumption rates for hydrogen and nitrogen (i.e., large-magnitude negative generation values). As the reaction proceeds along the reactor, the generation rate of ammonia and the consumption rates of hydrogen and nitrogen per unit length of reactor decrease. This is due to increasing the concentration of ammonia, which reduces the reaction

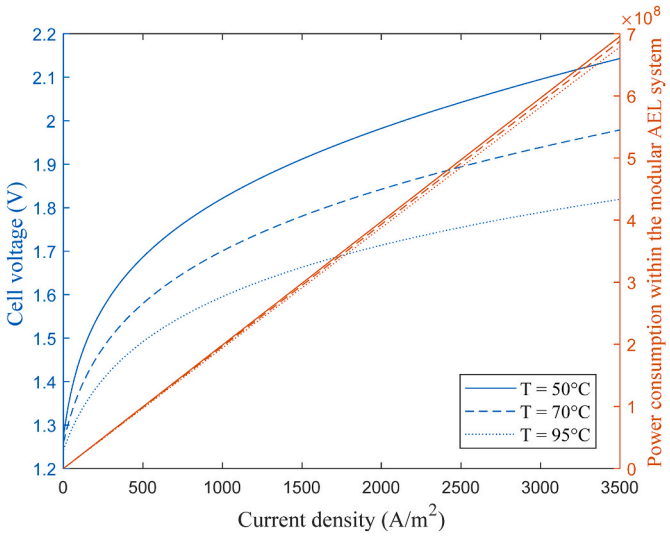

Fig. 4. V–I curve for the simulated AEL.

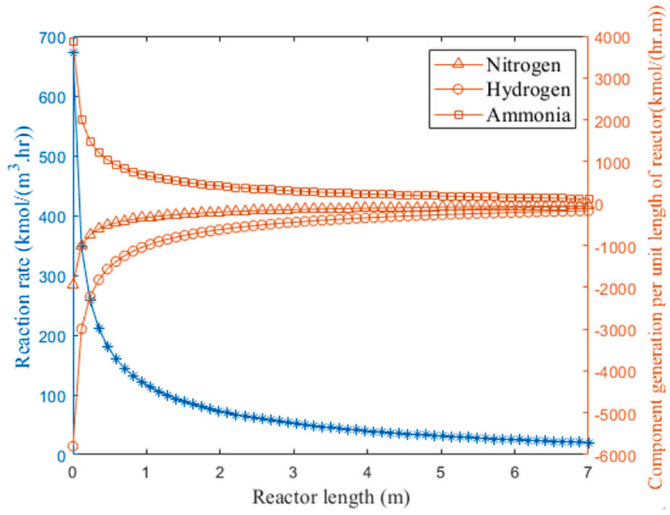

Fig. 5. Reaction rate, rate of reactants consumption and rate of ammonia production.

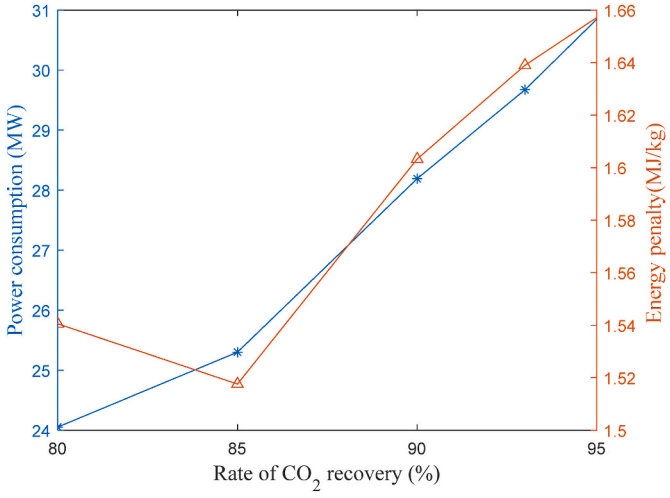

Fig. 6. Power consumption and energy penalty of CO_2 capture process.

rate. At the reactor outlet, the generation and consumption rates per unit length approach zero, reflecting the equilibrium conditions and a reaction rate that is almost zero.

Fig. 6 depicts the power consumption, and the energy penalty associated with the MEA scrubbing process without the HI for capturing CO_2 from a cement plant in Denmark, supplying it as a feedstock for the green urea production process. The values presented correspond to a system using a HP to meet the major portion of heat duty required for the regeneration of the solvent. Notably, the energy penalty values calculated in this study are slightly higher than those reported in the literature, primarily due to pressurizing the CO_2 stream to an exceptionally high pressure (139 bar) to meet the urea production requirements. As shown, the MEA scrubbing process has the lowest energy penalty when capturing 85 % of the CO_2 in the flue gas, as the system requires less energy per kilogram of captured CO_2. A similar trend was reported in Ref. [38]. However, increasing the CO_2 recovery rate from 85 % to 95 % significantly raises both power consumption and the energy penalty of the process. Specifically, the energy penalty and total power consumption increase by 9.19 % and 21.88 %, respectively. In this case, although more CO_2 is captured from the flue gas, the required heat duty for solvent regeneration increases more significantly because higher solvent flow rates are needed to separate the additional CO_2 from the gas mixture. To balance the power consumption and CO_2 emission costs, this study considers a CO_2 recovery rate of 90 %.

Fig. 7 illustrates the distribution of the specific electrical energy requirement (in $\frac{MJ_e}{kg_{CO_2}}$) among the different components involved in the MEA scrubbing process without the HI, namely blowers, compressors, and pumps, when capturing 90 % of the CO_2 emitted by the cement plant. In this setup, a HP provides the necessary heat duty for CO_2 desorption and solvent regeneration. As shown, the blowers, which pressurize the flue gas to compensate for the pressure drops within the MEA process, incur an energy penalty of 0.2495 $\frac{MJ_e}{kg_{CO_2}}$. This value aligns well with the specific power consumption range of 0.06–0.253 $\frac{MJ_e}{kg_{CO_2}}$ reported in Ref. [39]. The pumps contribute minimally to the overall power consumption, with a specific energy demand of approximately 0.007 $\frac{MJ_e}{kg_{CO_2}}$, close to the 0.00495 $\frac{MJ_e}{kg_{CO_2}}$ reported in Ref. [40]. The compressors, used both within the HP system and for pressurizing the CO_2 stream, exhibit the highest specific energy demand at 1.345 $\frac{MJ_e}{kg_{CO_2}}$. According to Ref. [39], the specific thermal energy required for solvent regeneration in an MEA scrubbing process is 3.882 $\frac{MJ}{kg_{CO_2}}$, while the specific electrical energy demand for CO_2 compression is 0.362 $\frac{MJ_e}{kg_{CO_2}}$.

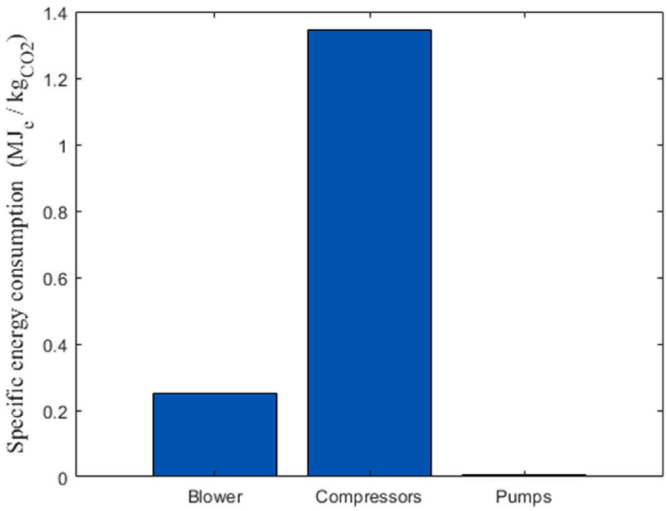

Fig. 7. The specific power demand across different components used in the MEA scrubbing process without HI.

Assuming a COP of 3.5 for the HP system, as cited in Ref. [41], the corresponding specific electrical energy demand for compressors within the MEA process presented in Ref. [39] would be approximately 1.47 $\frac{MJ_e}{kg_{CO_2}}$, which closely matches the value obtained in this study. The slight differences between the results obtained in this study and shown in Fig. 7 and those in the literature can be attributed to variations in component efficiencies (blowers, pumps, compressors), differences in CO_2 content in the flue gas, and the considered CO_2 recovery rates.

Fig. 8 illustrates the distribution of power consumption across the different subsystems depicted in Figs. 1 and 2 for sustainable urea production. As shown, whether the system includes the HI or not, the modular AEL unit accounts for the highest electricity consumption within the urea production process. It is worth noting that the MEA scrubbing process evaluated in this study requires a specific heat duty of 3.7 MJ per kilogram of captured CO_2 for solvent regeneration via CO_2 desorption. Integrating the 42.595 MW of waste heat generated from the ammonia production reactor into the stripper column for solvent regeneration reduces the power demand of the MEA scrubbing process by 50.54 %. This heat integration decreases the energy penalty associated with CO_2 capture from 1.603 MJ/kg_{CO_2} to 0.793 MJ/kg_{CO_2}.

Fig. 9 presents the specific energy requirements for urea production across the six scenarios outlined in Fig. 3. As shown, the specific energy consumption ranges from 22.97 to 24.5 $\frac{MJ}{kg_{urea}}$. The lowest energy requirement is observed for the scenario involving HP combined with HI, while the highest corresponds to natural gas combustion integrated with the CCC process without HI.

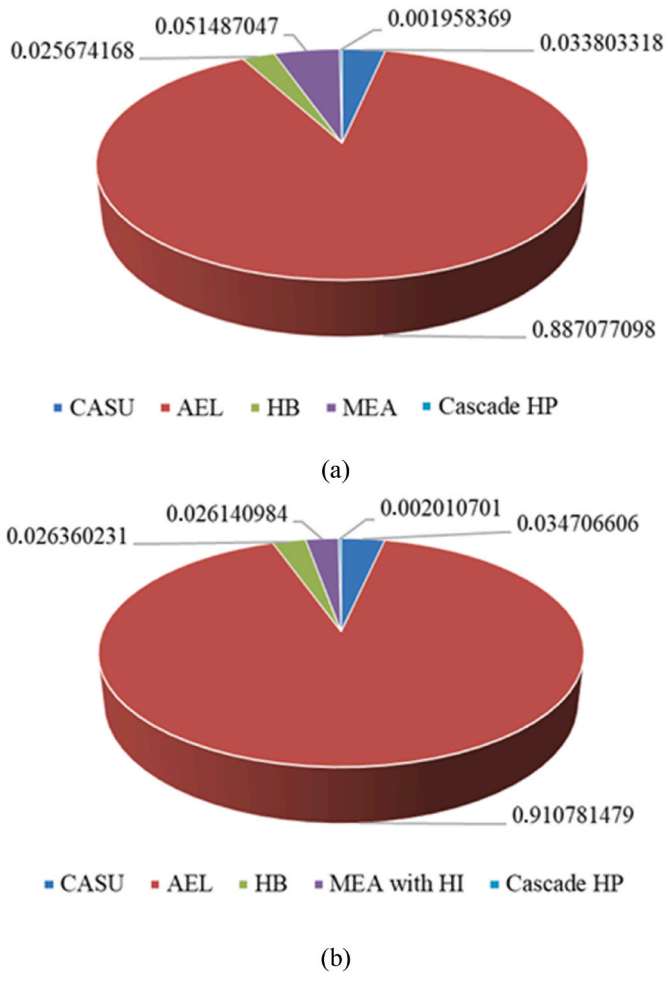

Fig. 8. The share of power consumption in different urea production subsystems (a) without (b) with HI.

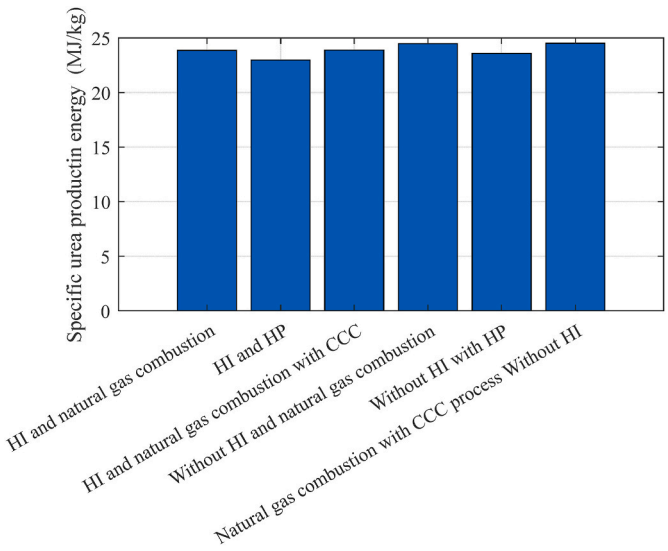

Fig. 9. Specific energy requirement for the urea production process.

3.2. Economic analysis

The studied cement factory does not operate year-round, as it requires six weeks of shortage for annual maintenance. The main outage, lasting three weeks, takes place during the last week of January and the first two weeks of February. The remaining three weeks of the short outages are scheduled as needed throughout the year. For this study, these short outages which each lasting 24 h are evenly distributed, occurring every 16 days in addition to the main outage. To calculate the electricity costs, the hourly electricity spot prices from 2022, 2023, and 2024 were used, as provided in the reference [42]. Table 4 summarizes the assumptions made for the economic analysis of the urea production process shown in Fig. 2.

As shown in Fig. 8, the implemented HI significantly reduces the power consumption in the MEA scrubbing process and enhances the system's energy efficiency. Under this situation, the HP will no longer be required for solvent regeneration. The heat duty can be supplied by the ammonia production reactor, along with the thermal energy provided by the hot flue gas stream and the pressurized CO_2 stream, which together meet the heat demand for CO_2 desorption and solvent regeneration. Consequently, as depicted in Fig. 10, the CO_2 capture costs for the MEA scrubbing process, applied to the flue gas from a cement plant, can be substantially lowered using this HI. Notably, in addition to the electricity costs, O&M costs and water-cooling costs were also considered in calculating the CO_2 capture costs using the MEA scrubbing process.

Table 4
Key assumptions for economic analysis of the urea production process

Operating and maintenance (O&M) costs		2.5 % of the initial investment costs [29]
Fresh water costs		0.35 $/ton [27]
The costs of deionized water costs		2 $/ton [29]
Selling point of the captured CO_2 in liquid phase		17.3 $/ton [43]
CO_2 emission tax in Europe in 2022, 2023, and 2024		24.04 €/ton [44]
Selling point of generated O_2 as a by-product of modular AEL system and CASU		150 €/ton [45]
Cost of iron-based catalyst for ammonia synthesis reactor		0.18 $/kg [3]
Natural gas price	2022	40.3 USD/MMBTU [46]
	2023	13.1 USD/MMBTU [46]
	2024	9.5 USD/MMBTU [46]

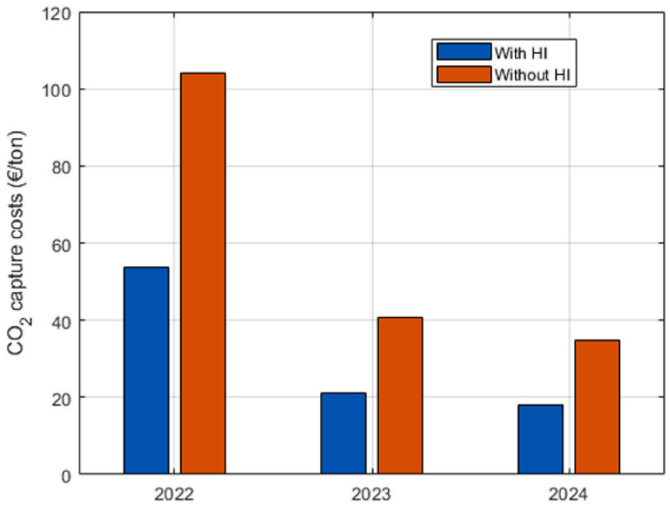

Fig. 10. The impact of heat integration on the CO_2 capture costs from the cement factory in the years 2022, 2023 and 2024.

As previously mentioned, the MEA scrubbing process is designed to capture 90 % of the CO_2 emissions from the cement factory, aiming to reduce CO_2 emission costs and avoid excessively high power consumption during the capture process. Fig. 11 illustrates the CO_2 emissions and the associated costs per ton of generated urea under three different scenarios for supplying the necessary heat and steam for the CO_2 stripper column in the Stamicarbon process: using cascade HP, integrating natural gas combustion with the CCC process (where 90 % of emitted CO_2 is captured), and relying solely on natural gas combustion. As shown in the figure, utilizing the cascade HP powered by renewable energy results in the lowest CO_2 emissions, whereas natural gas combustion leads to the highest CO_2 emissions and, consequently, the highest emission costs. When using the HP to supply the required heat for the CO_2 stripper column, no CO_2 is emitted, resulting in minimal CO_2 emission costs for the urea production process. Although integrating the CCC process with natural gas combustion reduces CO_2 emissions, it captures 90 % of the CO_2 because the concentration of CO_2 in the flue gas is very low. Achieving higher capture rates would lead to excessively high power consumption in the CCC process despite its high energy efficiency. While integrating natural gas combustion with the CCC process results in higher CO_2 emissions compared to the cascade HP, the overall CO_2 emission costs remain significantly lower than those of natural gas

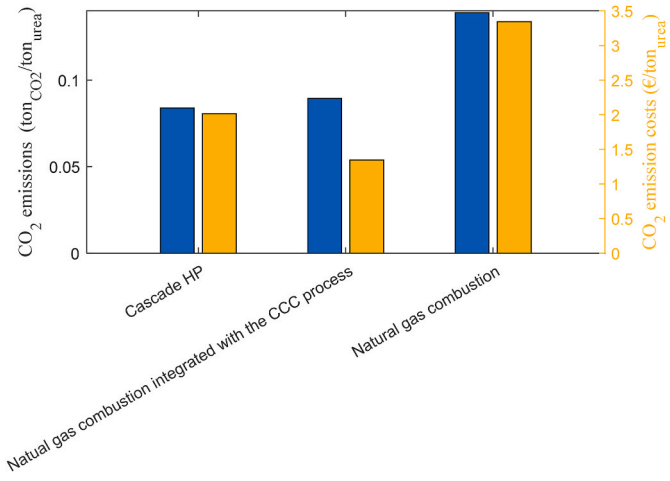

Fig. 11. CO_2 emission and CO_2 emission costs when using cascade HP, natural gas combustion with and without integration with the CCC process to supply the required heat for the urea production.

combustion without CO_2 capture. This cost reduction is due not only to lower emissions and reduced CO_2 taxes but also to the revenue generated from selling the captured CO_2 in liquid form with high purities (>99.9 %), which effectively offsets the emission costs.

Fig. 12 also illustrates the contribution of various factors to the costs of sustainable urea production across six scenarios in 2022, 2023, and 2024. These factors include electricity costs, O&M costs, water cooling costs, natural gas costs, deionized water costs, revenue from oxygen generation within the CASU and AEL modular system, and CO_2 emission costs. As shown in the figure, electricity costs have the highest share in the sustainable urea production process over the three evaluated years, primarily due to the exceptionally high power consumption of the modular AEL system. Consequently, urea production costs were significantly higher in 2022, driven by the elevated electricity spot price in that year. Additionally, selling the generated oxygen can substantially reduce the urea production costs, as a large volume of high-purity oxygen (0.971 ton_{O_2}/ton_{urea}) is produced within the urea production process shown in Figs. 1 and 2. It is also worth noting that the costs associated with fresh water for cooling, deionized water, and CO_2 emissions have only a minor impact on the overall urea production costs. As shown in Fig. 12, the scenario utilizing HP with HI is the most cost-effective, due to its slightly lower O&M costs and reduced electricity expenses (resulting from the omission of the HP within the MEA scrubbing process), and minimal CO_2 emission costs (since no CO_2 emissions occur when the required heat for the CO_2 stripper column is supplied), compared to the other scenarios. Additionally, it does not consume natural gas, resulting in zero natural gas costs. As shown in Fig. 12, implementing the HI has a noticeable impact on reducing the urea costs. However, integrating the CCC process when using the natural gas combustion to supply the required steam for the CO_2 stripper column does not significantly affect the urea production costs. Although the CCC process is considered one of the most energy-efficient methods for CO_2 capture and sequestration, the low CO_2 concentration (9.47 % vol%) in the flue gases generated by natural gas combustion negatively impacts its energy efficiency. More importantly, the amount of natural gas required to generate steam for the urea production process is minimal, resulting in relatively low CO_2 emissions (0.055 tons of CO_2 per ton of urea without CCC integration). Consequently, integrating the CCC process does not notably affect the overall urea production costs when using natural gas combustion for generating the required steam for Stamicarbon process.

According to Fig. 12, the sustainable urea price ranges from €351.83 to €372.96 per ton of urea, depending on the production scenario. These results are consistent with the costs reported in Ref. [47], which range from $268 to $413 per ton of urea.

Fig. 13 illustrates the breakdown of electricity costs in 2022, which, as shown in Fig. 12, represent the largest share of the urea production costs across the six scenarios analyzed in this study. According to Fig. 13, the modular AEL system is responsible for 88.74 %–91.26 % of the electricity costs throughout the entire urea production process, depending on the specific scenario. Additionally, as seen in this figure, both the CCC process and the cascade HP have an exceptionally low share in the electricity costs. This is due to the high energy efficiency of these two technologies, as well as their comparatively low load when generating sustainable urea. Following the AEL system, the MEA scrubbing process for capturing CO_2 from the cement plant (without the use of HI) has the highest share in the electricity costs of the urea production process.

Table 5 presents the breakdown of component costs used to calculate the initial investment costs for the urea production process shown in Fig. 2. It is important to note that the component costs listed in Table 5 were calculated using the Aspen Process Economic Analyzer (APEA). Although the equipment costs for the urea production process using the HI and HP scenario (as shown in Fig. 2) are presented in Table 5, this study employed APEA to estimate the equipment costs for the CCC process and natural gas combustion process which are used in the

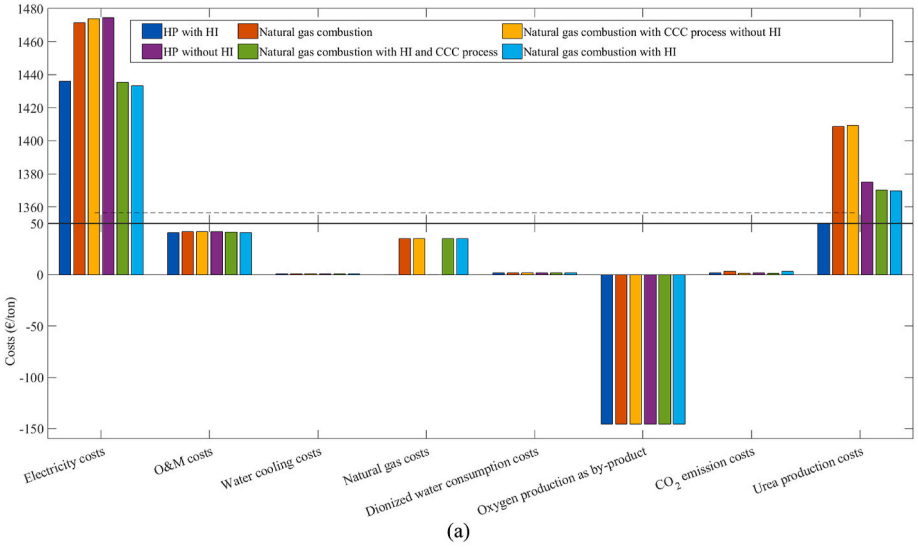

(a)

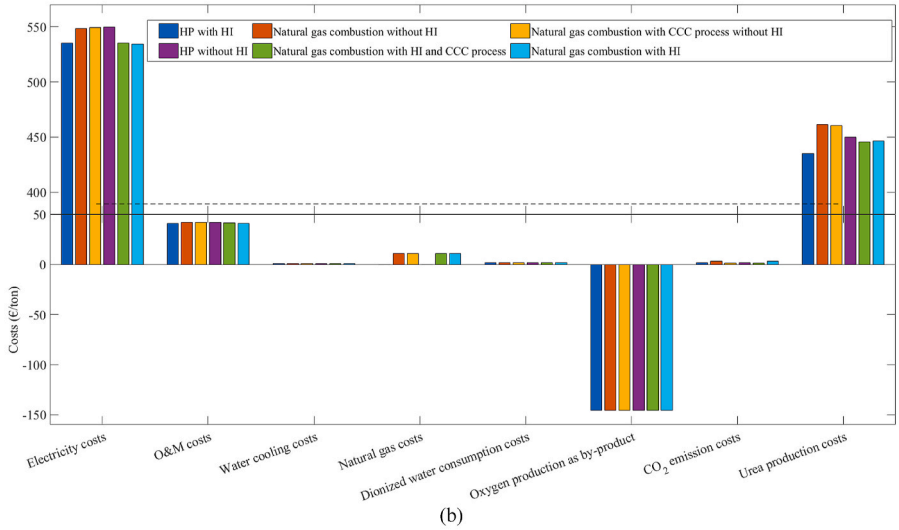

(b)

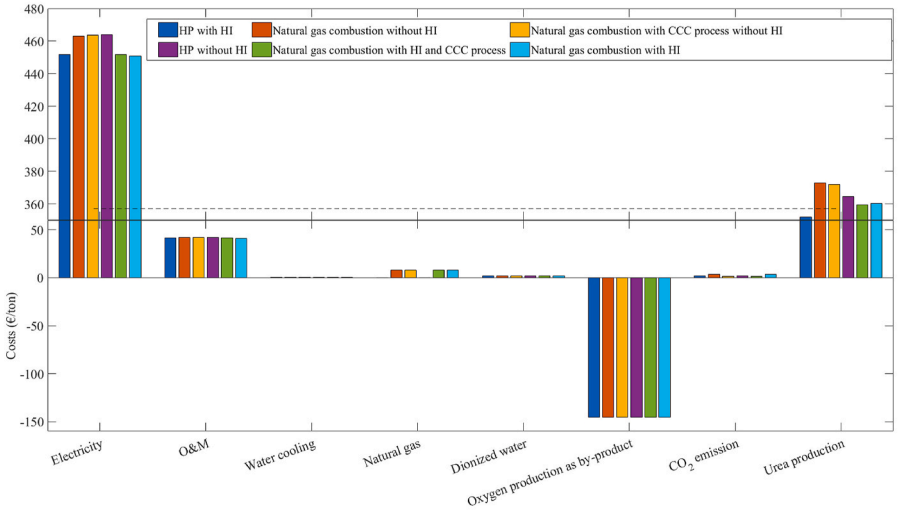

(c)

Fig. 12. Urea production costs considering the impact of different components in (a) 2022, (b) 2023, (c) 2024.

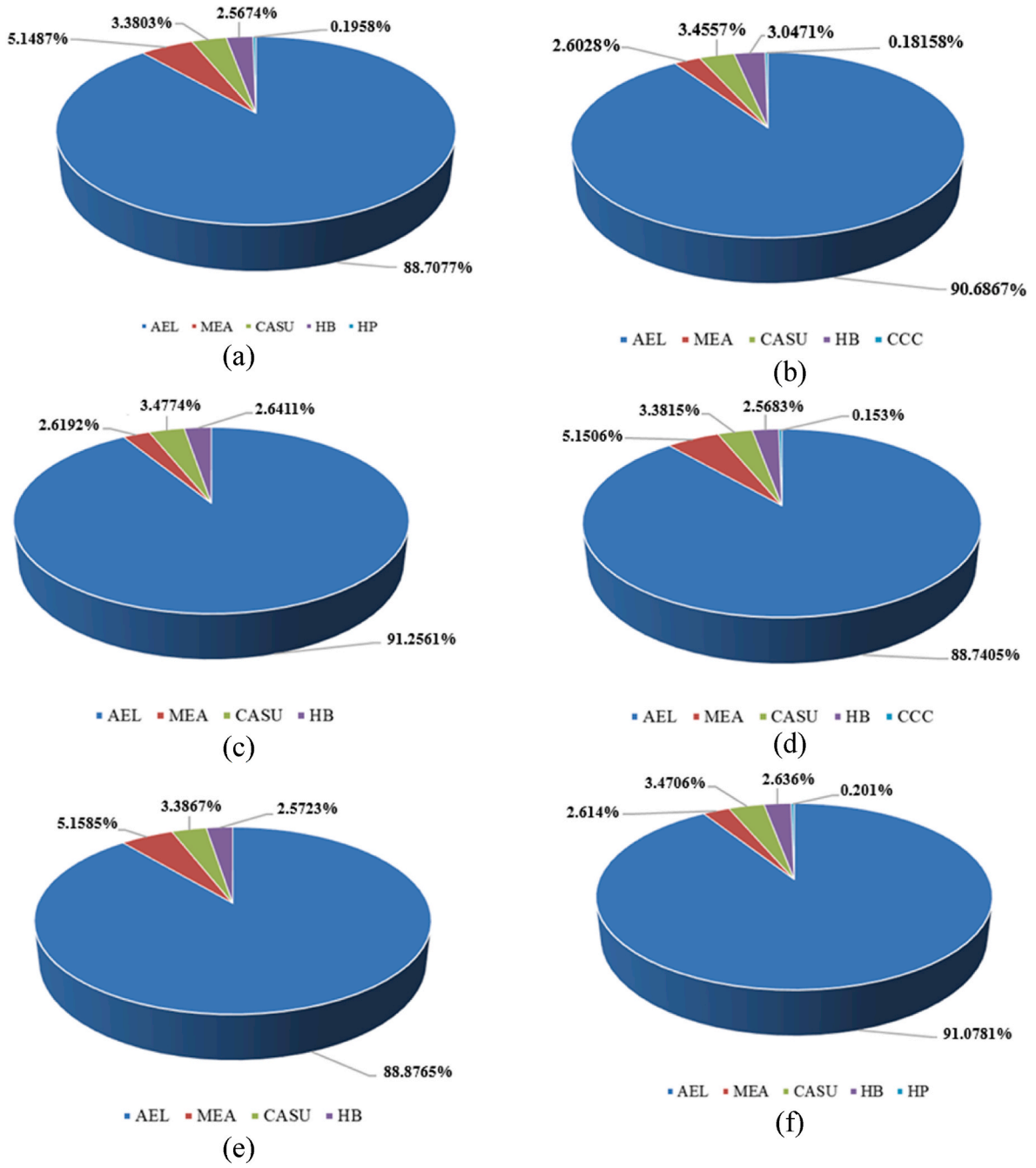

Fig. 13. The share of different components for electricity costs in sustainable urea production process when (a) using HP without HI (b) natural gas combustion with HI and the CCC process (c) natural gas combustion with HI (d) natural gas combustion with CCC process without HI (e) natural gas combustion without HI (f) HP with HI in 2022.

remaining scenarios. These estimates were subsequently used to calculate the O&M costs, as illustrated in Fig. 12. The APEA has been widely used in numerous studies to estimate the equipment costs for the chemical processes, and it is recognized as an accurate and reliable software tool for estimating the initial investment costs of these processes [48]. In estimating the component costs, the APEA uses flowsheet data to calculate the equipment's weight both pre- and post-installation, taking into account factors like equipment size and chosen materials to provide precise cost estimates. As shown in Table 5, this study employs a Lang factor of 4.7 to estimate the costs of establishing the urea production plant shown in Fig. 2, based on the equipment costs estimated by the APEA.

Fig. 14 illustrates the share of different subsystems shown in Fig. 2, in the initial investment costs of the urea production process. When considering Figs. 13 and 14, it is evident that green hydrogen production using the AEL system makes the highest contribution to operating costs (primarily driven by electricity costs) as well as initial investment and O&M costs. Therefore, improving the efficiency of AEL systems to reduce their power consumption and lowering their initial investment costs would significantly impact the overall cost of sustainable urea production. Additionally, as shown in Fig. 14, both the Stamicarbon subsystem and the cascade HP have a minimal share in the initial investment costs of the urea production process.

Table 5
Breakdown of the equipment costs and total initial investment costs for establishing the urea production plant shown in Fig. 2.

Item	Costs (M€)
Cooling tower	6.0722
Pumps	1.169
Heat exchangers	8.192
Flash	2.461
Columns	6.943
Compressors	60.37
Blower	7.568
Multi-stream heat exchangers	1.22
Reactors	6.44
AEL	970.25
Total equipment costs	1070.6852
Total cost of complete plant	5032.2204

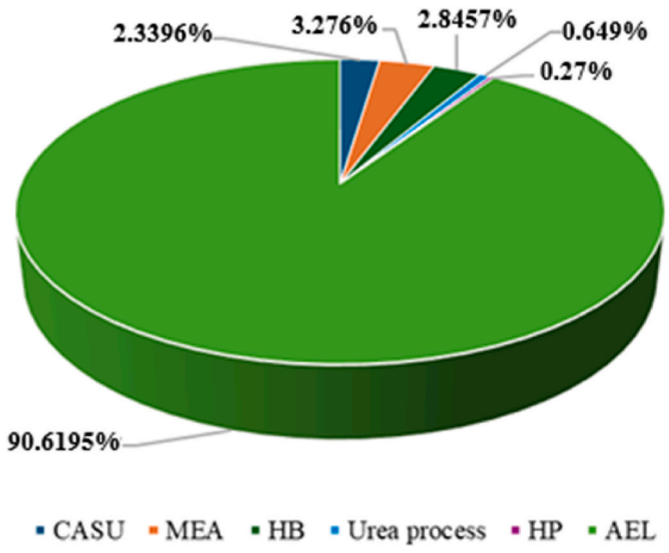

Fig. 14. Breakdown of CAPEX Components in the urea production process using HP with HI as the most cost-effective scenario.

4. Conclusion

This study conducted a comprehensive techno-economic analysis of sustainable urea production in Denmark, considering all subsystems involved, including AEL systems, CASU, the green HB process, the MEA scrubbing process for CO_2 capture from the cement plant, and the Stamicarbon process for converting the captured CO_2 and green ammonia into urea. To reduce the power consumption during the solvent regeneration in the MEA scrubbing process, this study integrated the exothermic heat generated in the ammonia production reactor of the green HB process into the MEA scrubbing system. Additionally, six different scenarios were evaluated to determine the most cost-effective method for sustainable urea production in 2022, 2023, and 2024. These scenarios included.

- Utilizing HI and a cascade HP to supply the required heat for the CO_2 stripper in the Stamicarbon process.
- Applying HP without HI.
- Using HI with natural gas combustion for steam production in the Stamicarbon process.
- Using HI and natural gas combustion integrated with the CCC process.
- Employing natural gas combustion without HI.
- Using natural gas combustion integrated with the CCC process without HI.

The results demonstrated that the first scenario, which employs HI and a cascade HP, is the most cost-effective method for sustainable urea production. Moreover, HI was found to significantly enhance the performance and energy efficiency of the MEA scrubbing process by reducing power consumption by 50.54 % and cutting its energy penalty from 1.603 MJ/kg_{CO_2} to 0.793 MJ/kg_{CO_2}. Consequently, the CO_2 capture cost in the MEA scrubbing process decreased by 46.85 %, from 35.543 €/ton to 18.89 €/ton in 2024, when using HI. This HI provides the main heating duty of 3.7 MJ per kilogram of captured CO_2 for solvent regeneration, corresponding to a total thermal energy of 42.595 MW. Additionally, the modular AEL system was identified as having the highest impact on sustainable urea production costs due to its substantial electricity costs, initial investment costs, and O&M expenses. Specifically, in 2022, the AEL modular system accounted for 91.08 % of electricity costs when using HP and HI for urea production, as well as 90.62 % of the initial investment costs under the same scenario. This study calculated the cost of green urea production, which ranges from €351.83 to €372.96 per ton of green urea, depending on the selected production scenario in Denmark.

This study evaluated the performance of urea production process under steady-state operating conditions, without considering the dynamic behavior of the sub-systems used in the green urea production. However, assessing this dynamic behavior is crucial when using intermittent renewable electricity to generate green urea, as each sub-system may respond differently to fluctuations in the power supply. To address this, Aspen Plus Dynamics can be used to evaluate the system's potential to operate with intermittent renewable electricity. Additionally, developing the transient model enables the evaluation of hydrogen storage's impact on the operating costs of green urea production and allows for an investigation of the operational flexibilities introduced by hydrogen storage.

CRediT authorship contribution statement

Hossein Asgharian: Writing – original draft, Visualization, Software, Methodology, Investigation, Formal analysis, Data curation, Conceptualization. **Albert Pujol Duran:** Writing – review & editing, Writing – original draft, Methodology, Investigation, Formal analysis, Conceptualization. **Ali Yahyaee:** Writing – review & editing, Software, Investigation. **Valeria Pignataro:** Writing – review & editing, Software, Investigation, Formal analysis. **Mads Pagh Nielsen:** Writing – review & editing, Supervision, Resources, Conceptualization. **Florin Iov:** Writing – review & editing, Resources, Methodology, Conceptualization. **Vincenzo Liso:** Writing – review & editing, Supervision, Software, Resources, Methodology, Funding acquisition, Conceptualization.

Declaration of competing interest

The authors declare that they have no known competing financial interests or personal relationships that could have appeared to influence the work reported in this paper.

Acknowledgement

The authors acknowledge the financial support from HySTrAm project, Grant Agreement Number 101058643.

Appendix A. Supplementary data

Supplementary data to this article can be found online at https://doi.org/10.1016/j.ijhydene.2025.150154.

References

[1] Fertilizer urea, food security, health a 1998;75(7):677–83.
[2] Statista. https://www.statista.com/statistics/1063689/global-urea-production-capacity/.
[3] Asgharian H, et al. Techno-economic analysis of blue ammonia synthesis using cryogenic CO2 capture Process-A Danish case investigation. Int J Hydrogen Energy Jun. 2024;69:608–18. https://doi.org/10.1016/j.ijhydene.2024.05.060.
[4] Devkota S, Karmacharya P, Maharjan S, Khatiwada D, Uprety B. Decarbonizing urea: techno-economic and environmental analysis of a model hydroelectricity and carbon capture based green urea production. Appl Energy Oct. 2024;372:123789. https://doi.org/10.1016/j.apenergy.2024.123789.
[5] Ghavam S, Vahdati M, Wilson IAG, Styring P. Sustainable ammonia production processes. Front Energy Res 2021;9(Mar). https://doi.org/10.3389/fenrg.2021.580808.
[6] María Villarreal Vives A, Wang R, Roy S, Smallbone A. Techno-economic analysis of large-scale green hydrogen production and storage. Appl Energy Sep. 2023;346:121333. https://doi.org/10.1016/j.apenergy.2023.121333.
[7] Mazzeo D, Herdem MS, Matera N, Wen JZ. Green hydrogen production: analysis for different single or combined large-scale photovoltaic and wind renewable systems. Renew Energy Nov. 2022;200:360–78. https://doi.org/10.1016/j.renene.2022.09.057.
[8] Ehlers JC, Feidenhans'l AA, Therkildsen KT, Larrazábal GO. Affordable green hydrogen from alkaline water electrolysis: key research needs from an industrial perspective. ACS Energy Lett Mar. 2023;8(3):1502–9. https://doi.org/10.1021/acsenergylett.2c02897.
[9] Galusnyak SC, Petrescu L, Cormos C-C. Environmental impact assessment of post-combustion CO2 capture technologies applied to cement production plants. J Environ Manage Oct. 2022;320:115908. https://doi.org/10.1016/j.jenvman.2022.115908.
[10] Alfian M, Purwanto WW. Multi-objective optimization of green urea production. Energy Sci Eng Apr. 2019;7(2):292–304. https://doi.org/10.1002/ese3.281.
[11] Gyanwali K, Karki S, Adhikari P, Devkota S, Aryal P. Techno-economic assessment of green urea production utilizing municipal solid waste and hydropower in Nepal. J Clean Prod Sep. 2023;419:138320. https://doi.org/10.1016/j.jclepro.2023.138320.
[12] Zhang H, Wang L, Van herle J, Maréchal F, Desideri U. Techno-economic comparison of 100% renewable urea production processes. Appl Energy Feb. 2021;284:116401. https://doi.org/10.1016/j.apenergy.2020.116401.
[13] Fernando C, Purwanto WW. Techno-economic analysis of a small-scale power-to-green urea plant. IOP Conf Ser Earth Environ Sci Mar. 2021;716(1):012010. https://doi.org/10.1088/1755-1315/716/1/012010.
[14] Kashyap TT, Sharma R, Paul D, Hiremath R. Techno-economic feasibility of CO2 utilization for production of green urea by Indian cement industries. J Clean Prod Oct. 2024;476:143799. https://doi.org/10.1016/j.jclepro.2024.143799.
[15] Guzmán RO, Lazo AB. Simulation of a reactor considering the Stamicarbon, Snamprogetti, and Toyo patents for obtaining urea. Open Chem Jan. 2022;20(1):424–30. https://doi.org/10.1515/chem-2022-0157.
[16] Diéguez PM, Ursúa A, Sanchis P, Sopena C, Guelbenzu E, Gandía LM. Thermal performance of a commercial alkaline water electrolyzer: experimental study and mathematical modeling. Int J Hydrogen Energy Dec. 2008;33(24):7338–54. https://doi.org/10.1016/j.ijhydene.2008.09.051.
[17] Eiga. Guideline for safe practices for cryogenic air separation plants. www.eiga.eu.
[18] Alie C, Backham L, Croiset E, Douglas PL. Simulation of CO2 capture using MEA scrubbing: a flowsheet decomposition method. Energy Convers Manag 2005;46(3):475–87. https://doi.org/10.1016/j.enconman.2004.03.003.
[19] Mullen D, Braakhuis L, Knuutila HK, Gibbins J, Lucquiaud M. Monoethanolamine degradation rates in post-combustion CO 2 capture plants with the capture of 100% of the added CO 2. Ind Eng Chem Res Aug. 2024;63(31):13677–91. https://doi.org/10.1021/acs.iecr.4c01525.
[20] Pujol A, Heuckendorff M, Pedersen TH. Techno-economic analysis of two novel Direct air capture-to-urea concepts based on process intensification. J Clean Prod Feb. 2025:144932. https://doi.org/10.1016/J.JCLEPRO.2025.144932.
[21] Zhang H, Wang L, Van herle J, Maréchal F, Desideri U. Techno-economic comparison of 100% renewable urea production processes. Appl Energy 2021;284(Feb). https://doi.org/10.1016/j.apenergy.2020.116401.
[22] Farahani SS, Rajabipour A, Keyhani A, Sharifi M. Energy use and economic analysis of NPK-15:8:15 fertilizer granulation process in Iran. J Saudi Soc Agricultural Sci Jul. 2017;16(3):265–9. https://doi.org/10.1016/J.JSSAS.2015.09.001.
[23] Shi L, Liu L, Yang B, Sheng G, Xu T. Evaluation of industrial urea energy consumption (EC) based on life cycle assessment (LCA). Sustainability May 2020;12(9):3793. https://doi.org/10.3390/SU12093793. 2020, Vol. 12, Page 3793.
[24] Meessen J. Urea synthesis. Chem Ing Tech 2014;86(12):2180–9. https://doi.org/10.1002/cite.201400064.
[25] Jensen MJ, et al. Prediction and validation of external cooling loop cryogenic carbon capture (CCC-ECL) for full-scale coal-fired power plant retrofit. Int J Greenh Gas Control Nov. 2015;42:200–12. https://doi.org/10.1016/j.ijggc.2015.04.009.
[26] Evans R. Pumping plant performance. https://content.ces.ncsu.edu/pumping-plant-performance?utm_source=chatgpt.com.
[27] Asgharian H, Iov F, Pagh Nielsen M, Liso V, Burt S, Baxter L. Analysis of cryogenic CO2 capture technology integrated with Water-Ammonia Absorption refrigeration cycle for CO2 capture and separation in cement plants. Sep Purif Technol Jan. 2025;353:128419. https://doi.org/10.1016/j.seppur.2024.128419.
[28] Sakas G, Ibáñez-Rioja A, Ruuskanen V, Kosonen A, Ahola J, Bergmann O. Dynamic energy and mass balance model for an industrial alkaline water electrolyzer plant process. Int J Hydrogen Energy Jan. 2022;47(7):4328–45. https://doi.org/10.1016/j.ijhydene.2021.11.126.
[29] Asgharian H, Pignataro V, Iov F, Pagh Nielsen M, Liso V. Exceeding equilibrium limitations: enhanced temperature control for sustainable decentralized green ammonia production – a techno-economic analysis. Energy Convers Manag Sep. 2024;315:118764. https://doi.org/10.1016/j.enconman.2024.118764.
[30] S R, Li B, Zhang N. Rate-based modelling of CO2 capture process by reactive absorption with MEA. Chem Eng Trans 2014;39:13–8.
[31] Hikita H, Asai S, Ishikawa H, Honda M. The kinetics of reactions of carbon dioxide with monoethanolamine, diethanolamine and triethanolamine by a rapid mixing method. Chem Eng J 1977;13(1):7–12. https://doi.org/10.1016/0300-9467(77)80002-6.
[32] Pinsent BRW, Pearson L, Roughton FJW. The kinetics of combination of carbon dioxide with hydroxide ions. Trans Faraday Soc 1956;52:1512. https://doi.org/10.1039/tf9565201512.
[33] Kibria MA, McManus DE, Bhattacharya S. Options for net zero emissions hydrogen from Victorian lignite. Part 2: ammonia production. Int J Hydrogen Energy Dec. 2023;48(95):37166–82. https://doi.org/10.1016/j.ijhydene.2023.06.098.
[34] Hamidipour M, Mostoufi N, Sotudeh-Gharebagh R. Modeling the synthesis section of an industrial urea plant. Chem Eng J Feb. 2005;106(3):249–60. https://doi.org/10.1016/j.cej.2004.12.020.
[35] Hamidipour M, Mostoufi N, Sotudeh-Gharebagh R. Modeling the synthesis section of an industrial urea plant. Chem Eng J Feb. 2005;106(3):249–60. https://doi.org/10.1016/j.cej.2004.12.020.
[36] Miles MH, Kissel G, Lu PWT, Srinivasan S. Effect of temperature on electrode kinetic parameters for hydrogen and oxygen evolution reactions on nickel electrodes in alkaline solutions. J Electrochem Soc Mar. 1976;123(3):332–6. https://doi.org/10.1149/1.2132820.
[37] Lohmann-Richters FP, Renz S, Lehnert W, Müller M, Carmo M. Review—challenges and opportunities for increased current density in alkaline electrolysis by increasing the operating temperature. J Electrochem Soc Nov. 2021;168(11):114501. https://doi.org/10.1149/1945-7111/ac34cc.
[38] Rao AB, Rubin ES. Identifying cost-effective CO 2 control levels for amine-based CO 2 capture systems. Ind Eng Chem Res 2006;45(8):2421–9. https://doi.org/10.1021/ie050603p.
[39] Adu E, Zhang YD, Liu D, Tontiwachwuthikul P. Parametric process design and economic analysis of post-combustion CO2 capture and compression for coal- and natural gas-fired power plants. Energies May 2020;13(10):2519. https://doi.org/10.3390/en13102519.
[40] Li K, Leigh W, Feron P, Yu H, Tade M. Systematic study of aqueous monoethanolamine (MEA)-based CO2 capture process: techno-economic assessment of the MEA process and its improvements. Appl Energy Mar. 2016;165:648–59. https://doi.org/10.1016/j.apenergy.2015.12.109.
[41] Staffell I, Brett D, Brandon N, Hawkes A. A review of domestic heat pumps. Energy Environ Sci 2012;5(11):9291. https://doi.org/10.1039/c2ee22653g.
[42] Energy-Charts. Electricity production and spot prices in Denmark. https://energy-charts.info/charts/price_spot_market/chart.htm?l=en&c=DK&year=2024.
[43] Zang G, Sun P, Elgowainy AA, Bafana A, Wang M. Performance and cost analysis of liquid fuel production from H2and CO2based on the Fischer-Tropsch process. J CO2 Util 2021;46(February):101459. https://doi.org/10.1016/j.jcou.2021.101459.
[44] Mehta D, Prajapati P. Asymmetric effect of environment tax and spending on CO2 emissions of European Union. Environ Sci Pollut Control Ser 2024;31(18):27416–31. https://doi.org/10.1007/s11356-024-32990-y.
[45] Bellotti D, Rivarolo M, Magistri L, Massardo AF. Thermo-economic comparison of hydrogen and hydro-methane produced from hydroelectric energy for land transportation. Int J Hydrogen Energy Feb. 2015;40(6):2433–44. https://doi.org/10.1016/j.ijhydene.2014.12.066.
[46] Natural gas commodity prices in Europe and the United States from 1980 to 2024, with a forecast for 2025 and 2026. https://www.statista.com/statistics/252791/natural-gas-prices/.
[47] Soroodan E, Huang S, Milani D, Kiani A, Feron P. Techno-economic assessment of green urea production integrated with direct air capture. Energy Convers Manag X Apr. 2025;26:101015. https://doi.org/10.1016/j.ecmx.2025.101015.
[48] Sultan H, Bhatti UH, Muhammad HA, Nam SC, Baek IH. Modification of postcombustion CO 2 capture process: a techno-economic analysis. Greenhouse Gases: Sci Technol Feb. 2021;11(1):165–82. https://doi.org/10.1002/ghg.2042.